

Dépôt de nano-aimants préformés : des propriétés intrinsèques à l'auto-organisation

F. Tournus

Groupe « Nanostructures magnétiques »

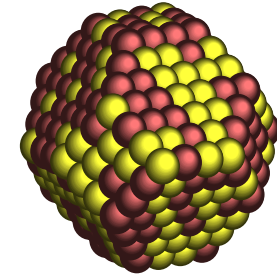
Institut Lumière Matière, UMR 5306 CNRS & Univ. Lyon 1

- Motivations
- Cluster deposition: originality of the LECBD technique
- CoPt nanoparticles: chemical order and magnetic anisotropy?
 - ✓ Magnetic measurements
 - ✓ Structural characterization
- Self-organization of Pt based nanoparticles on C substrates
 - ✓ Clusters deposited on graphite and carbon nanotubes
 - ✓ Pt cluster organized on graphene/Ir(111)
- Perspectives

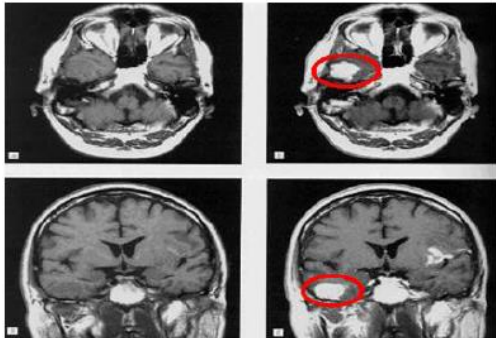
Small nanoparticles ($D < 5 \text{ nm}$)

Size reduction effect (major importance of the surface)

➔ The properties can differ from the bulk ones



2.7 nm diameter cluster (586 atoms):
45% of the atoms on the surface



- Biological/medical applications
 - ✓ Targeted drug delivery
 - ✓ Hyperthermia (cancer treatment)
 - ✓ MRI contrast agent

- Catalysis

- Spintronic devices

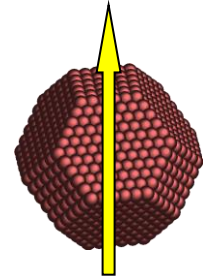
- Magnetic storage applications

➔ High density storage ($> 1 \text{ Tb/inch}^2$)



Ferromagnetic nanoparticle as an ultimate bit of information

Monodomain particle = macrospin



Problem: **superparamagnetism**

➡ Magnetization fluctuation in nanostructures

Energy barrier to switch the magnetization

➡ Magnetic anisotropy energy: $E_{\text{ani}} = K_{\text{eff}} V$ (K_{eff} is the anisotropy constant)

It controls the stability (temporal, thermal, magnetic) of nanomagnets

Magnetization switching frequency: $\nu = \nu_0 \exp(-E_{\text{ani}} / k_B T)$

Ex.: for a 3 nm diameter Co particle, the magnetic moment switches each 2 ns

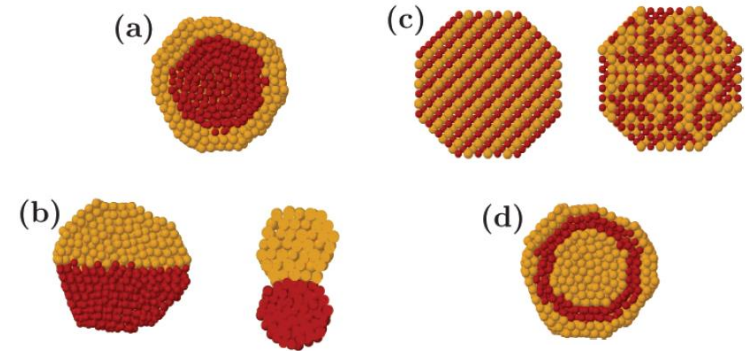
Stable nanomagnets (magnetic storage) ➡ Increase K_{eff}

✓ Surface/interface effect

✓ Volume effect (cluster structure, composition) ➡ Alloys

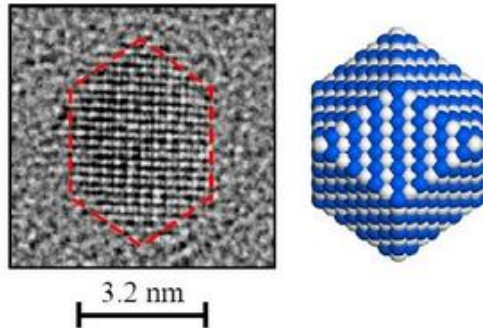
➔ Two types of atoms:
additional degree of freedom

➔ Nanoalloys, bimetallic particles:
different types of structures



New properties, combination of properties, at the nanoscale

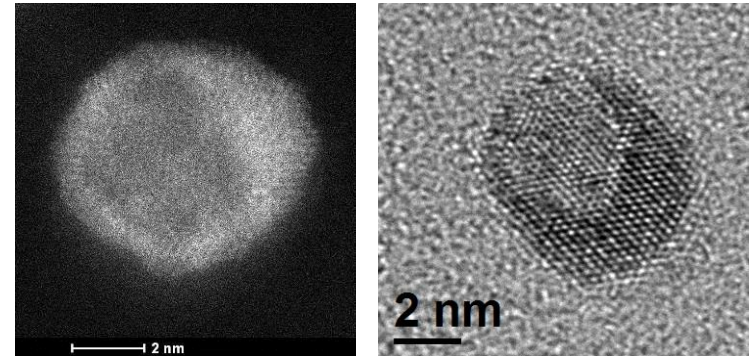
Ex. FeRh



Ferromagnetic order stable at low T
(instead of anti-ferromagnetic)

A. Hillion *et al.*, Phys. Rev. Lett. **110**, 087207 (2013)

Ex. CoAu

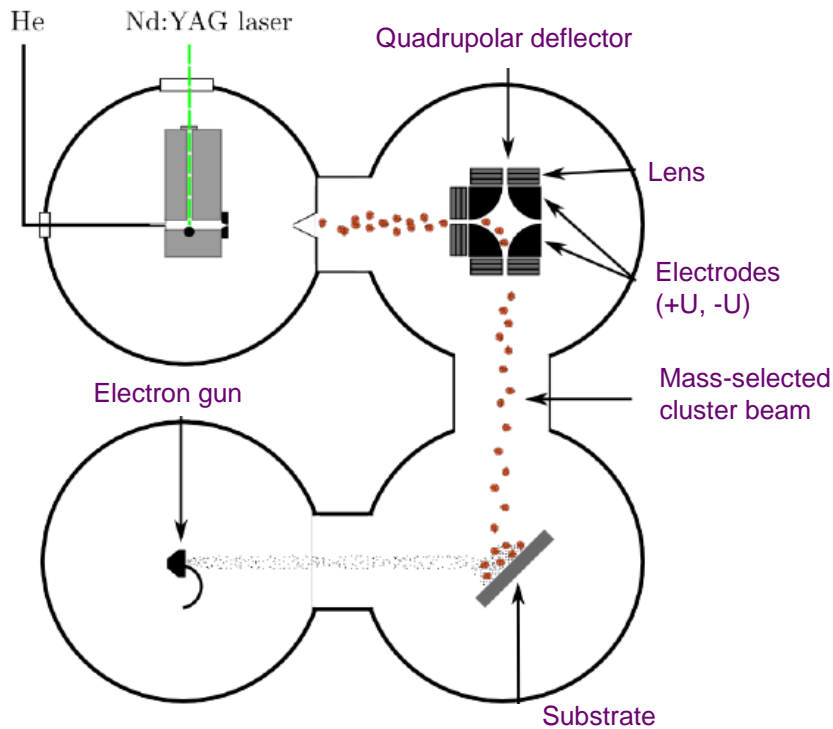


Original structures, magneto-plasmonic interest

Our general research axis: link between the structure (including the particles environment) and the magnetic properties.

- Motivations
- **Cluster deposition: originality of the LECBD technique**
- CoPt nanoparticles: chemical order and magnetic anisotropy?
 - ✓ Magnetic measurements
 - ✓ Structural characterization
- Self-organization of Pt based nanoparticles on C substrates
 - ✓ Clusters deposited on graphite and carbon nanotubes
 - ✓ Pt cluster organized on graphene/Ir(111)
- Perspectives

Deposition of preformed clusters (physical route)



Low energy cluster beam deposition, based on a laser vaporization source

- ✓ Deposition under ultra-high vacuum
- ✓ Adjustable composition (target)
- ✓ Capping or co-deposition in a matrix
 - ➔ • Protect the particles
 - Avoid coalescence

- ✓ Possibility of size selection (quadrupolar electrostatic deflector)

All the particles have the same velocity

- ➔ Selection of kinetic energy = mass selection

A. Perez *et al.*, *Int. J. Nanotechnol.* **7**, 523 (2010)

R. Alayan *et al.*, *Rev. Sci. Instrum.* **75**, 2461 (2004)

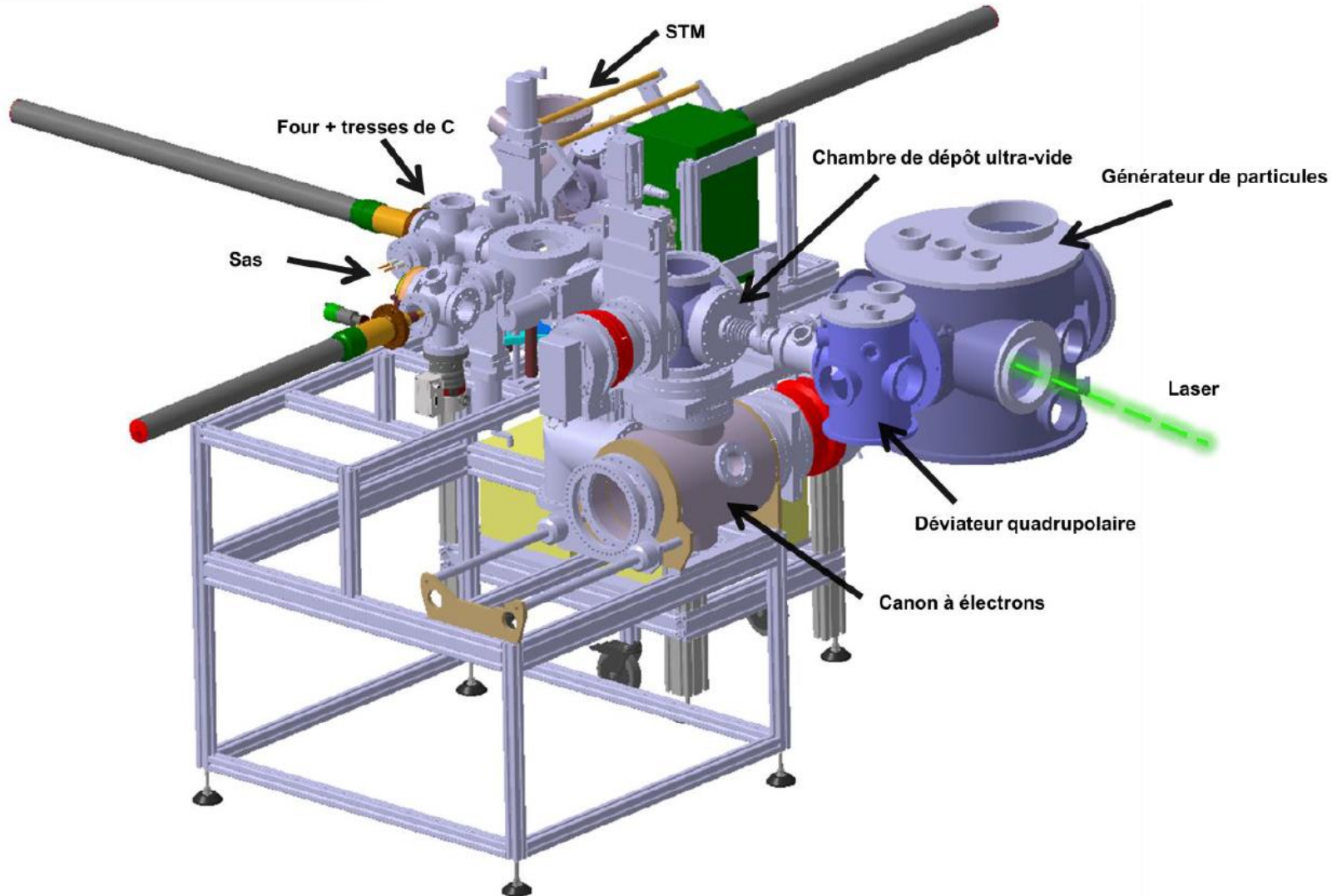


Figure I-4 : Représentation 3D de la source triée en taille.

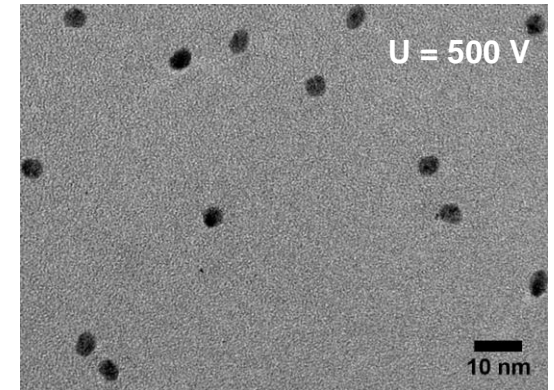
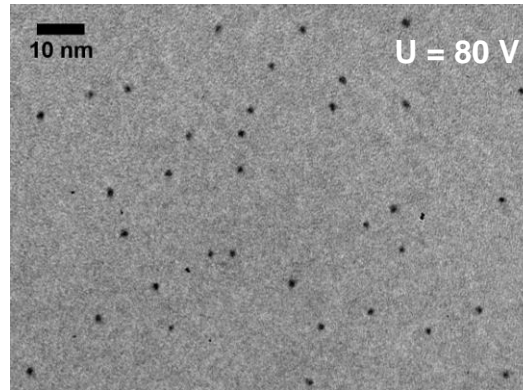
Typical nanoparticle diameter ~ 3 nm

- Adjustable particle size, independently from the surface density.

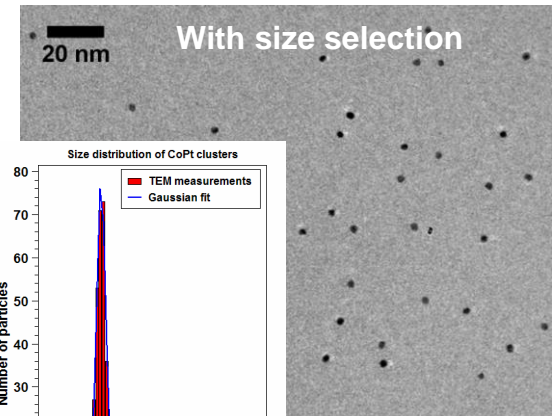
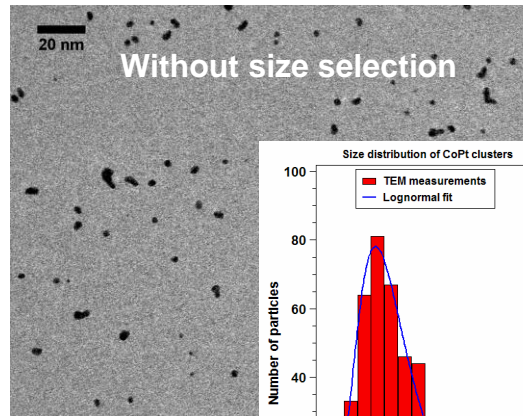


Diluted assemblies (avoid interactions)

- Relative diameter dispersion lower than 10 % with size selection.
- Random deposition.



CoPt nanoparticles

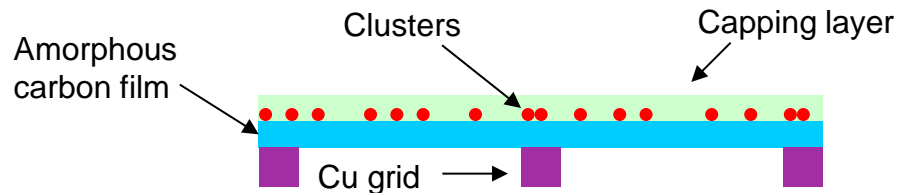


$$\Delta D/D_m \sim 7-8 \%$$

✓ 2D cluster films

➔ With or without a capping layer

For example, for TEM studies, with an amorphous carbon capping.

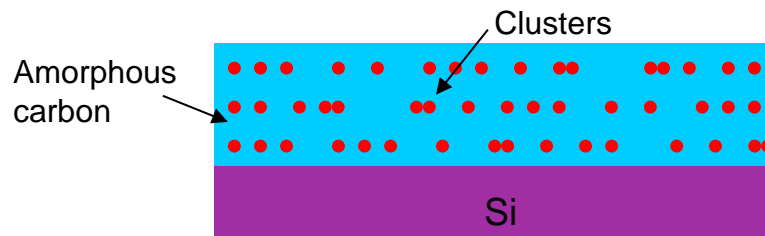


✓ Multilayers (“Mille-feuille”)

Diluted 2D cluster layer:

➔ { Equivalent thickness $\sim 0.5 \text{ \AA}$
Mean interparticle distance $\sim 10 \text{ nm}$

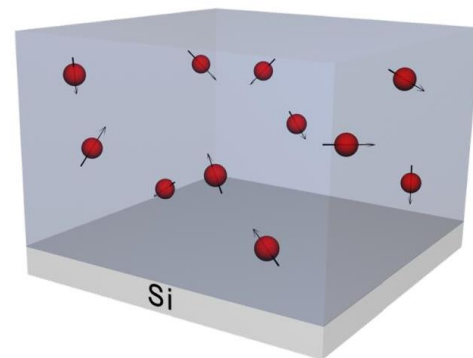
Matrix as a spacer.



For example, for magnetic measurements.

✓ Diluted 3D assemblies

Clusters embedded in a co-deposited matrix.



This approach allows ex-situ characterization by many techniques (EXAFS, XRD, XMCD, TEM, SQUID...)

Very sensitive method to detect magnetic interactions

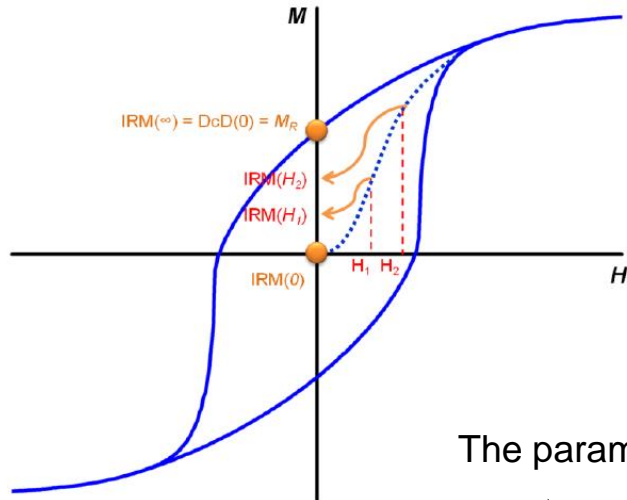
Isothermal remanence magnetization (IRM):

Starting from a demagnetized state, measurement at remanence after application of a magnetic field H .

➡ Irreversible switching of some macrospins.

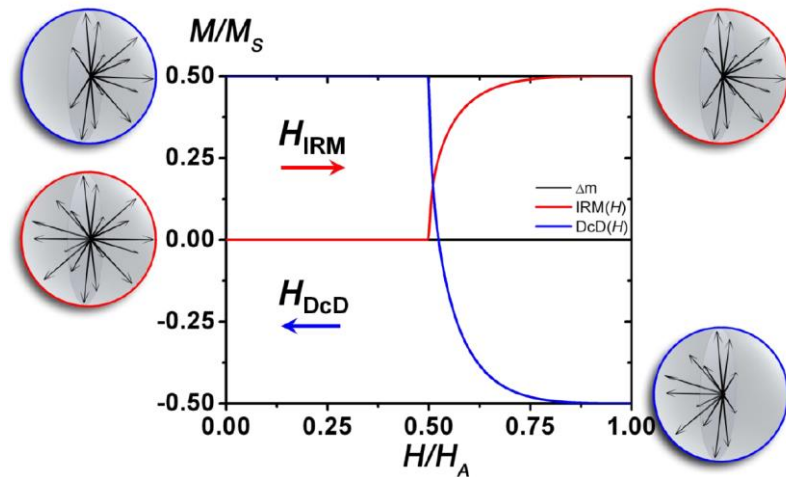
Dc demagnetization (DcD):

Same as IRM, but starting from m_R (after saturation).

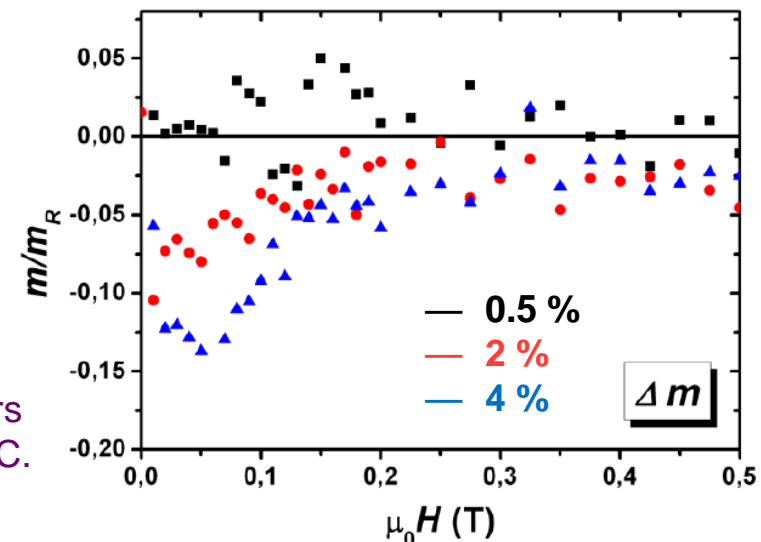


The parameter $\Delta m = DcD(H) - (m_R - 2 IRM(H))$ is equal to zero with no interaction.

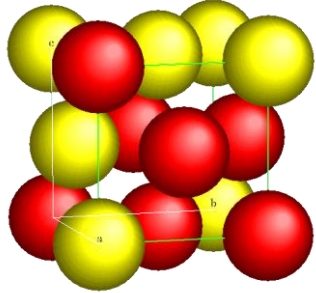
➡ With a volume concentration $< 1\%$, interactions are negligible.



Purple clusters diluted in C.

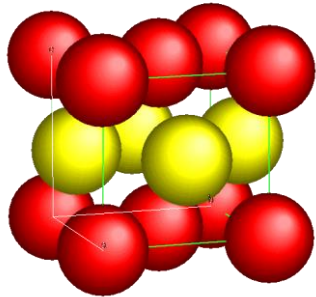


- Motivations
- Cluster deposition: originality of the LECBD technique
- **CoPt nanoparticles: chemical order and magnetic anisotropy?**
 - ✓ Magnetic measurements
 - ✓ Structural characterization
- Self-organization of Pt based nanoparticles on C substrates
 - ✓ Clusters deposited on graphite and carbon nanotubes
 - ✓ Pt cluster organized on graphene/Ir(111)
- Perspectives



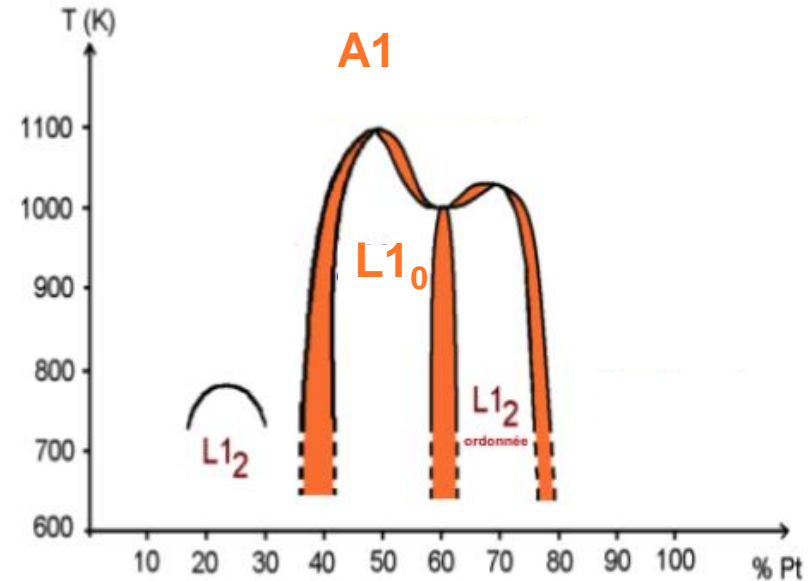
A1 phase

- Chemically disordered
- fcc cell



L₁₀ phase

- Chemically ordered
- tetragonal cell ($c/a < 1$)



Phase diagram for the bulk

The L₁₀ phase has an extremely high magnetic anisotropy constant ($K_{\text{eff}} \sim 5 \text{ MJ/m}^3$)

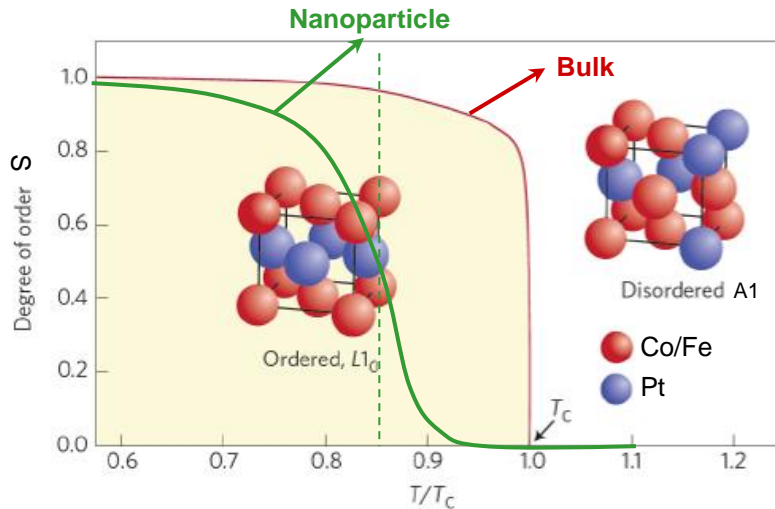
➡ Magnetocrystalline anisotropy (due to the Co/Pt stacking)

Common feature to 3d-5d magnetic alloys (FePt etc.)

The L₁₀ phase is the stable one at room temperature, but A1 is metastable

- Chemical ordering by annealing

➔ Synthesis itself is a challenge (well defined size, no coalescence, no pollution...)

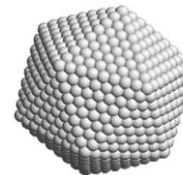


- Chemical order phase transition shifted and smoothed for nano-sizes

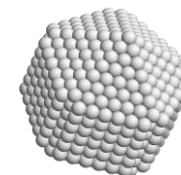
➔ Threshold size for the stability of the $L1_0$ phase?

D. Alloyeau *et al.*, *Nature Mater.* **8**, 940 (2009) ;
K. Sato, *Nature Mater.* **8**, 924 (2009).

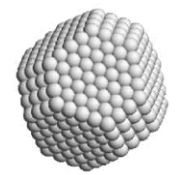
- As a function of size, competition between different geometries



Icosahedron



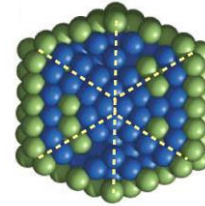
Decahedron



Truncated octahedron

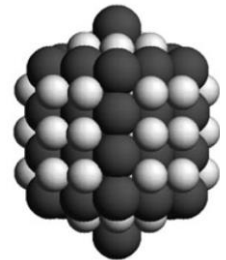
- Several theoretical predictions

➔ A decahedron with a “L1₀” order should be favorable

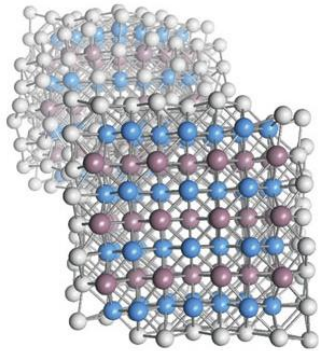


Core-shell icosahedron with depleted subsurface shell

M. Grüner *et al.*, *Phys. Rev. Lett.* **100**, 087203 (2008)



G. Rossi *et al.*
Faraday Discuss.
138, 193 (2008)

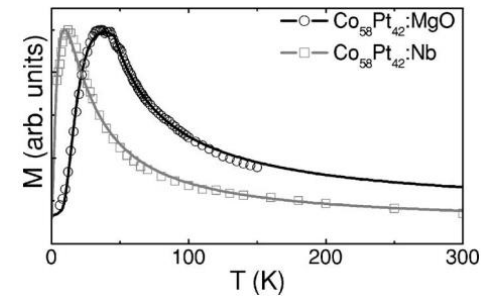


Fe₈₀Pt₆₇Al₁₆₂

- Influence of the environment (interface, magnetically dead layer, inter-particle interactions...)



Intrinsic properties of the nanoparticles?



S. Rohart *et al.*, *Phys. Rev. B* **74**, 104408 (2006).

The intrinsic magnetic properties of nano-sized chemically ordered CoPt particles are very difficult to determine reliably.

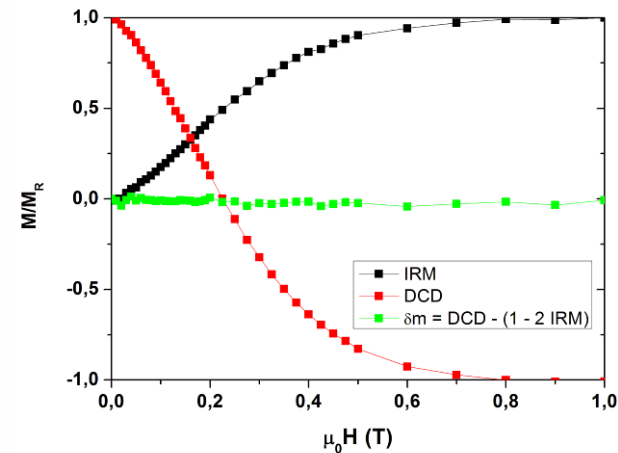
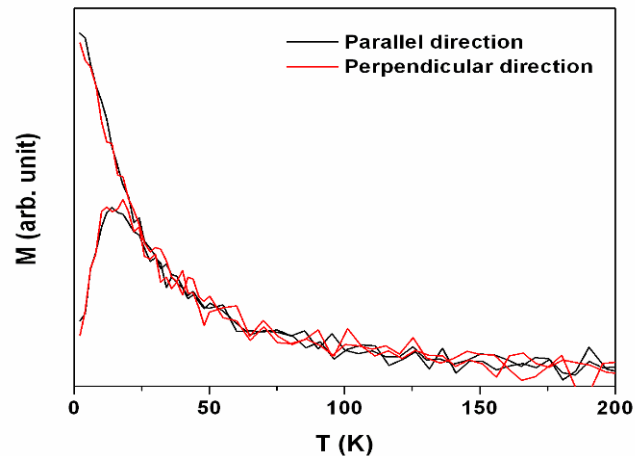
➔ Combine **structural** and **magnetic** characterizations of CoPt nanoparticles.

C. Antoniak *et al.*, *Nat. Commun.* **2**, 528 (2011).

✓ Magnetic measurements on CoPt particles

- CoPt nanoparticles embedded in an amorphous carbon matrix
- With or without size-selection
- Before and after annealing (2h at 750 K)
 - ➔ Promote chemical ordering

Verification of the absence of interactions

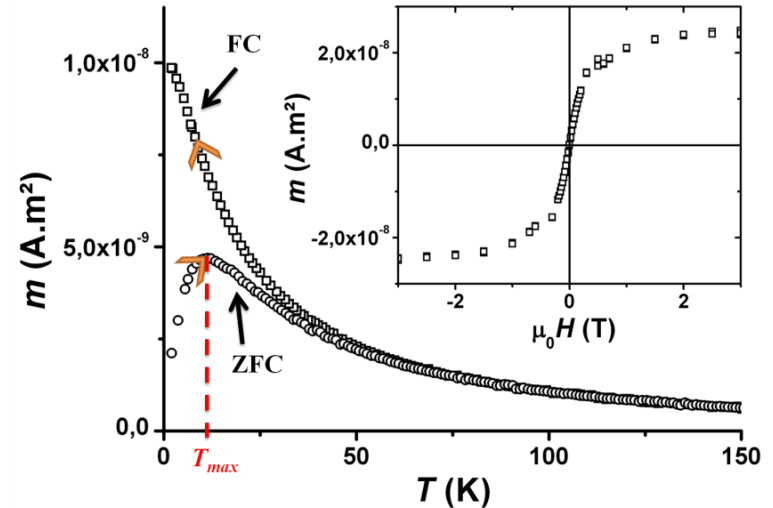


CoPt nanoparticles diluted in a carbon matrix

Low field susceptibility measurements:

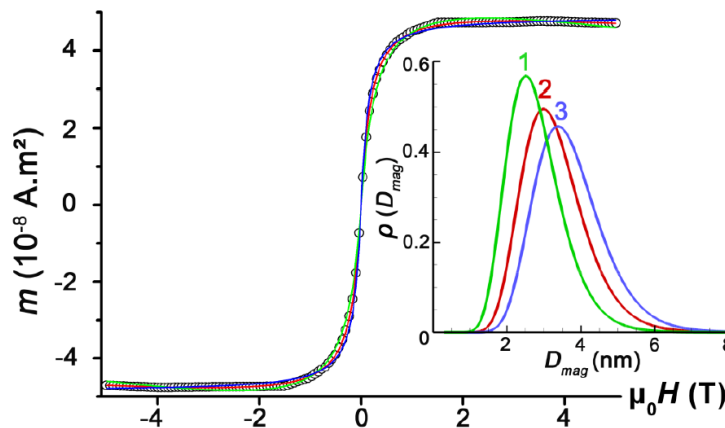
- ✓ Separation of the zero-field cooled (ZFC) and field-cooled (FC) curve
- ✓ ZFC peak at T_{max}

The particles, initially blocked, become superparamagnetic \rightarrow Magnetic anisotropy

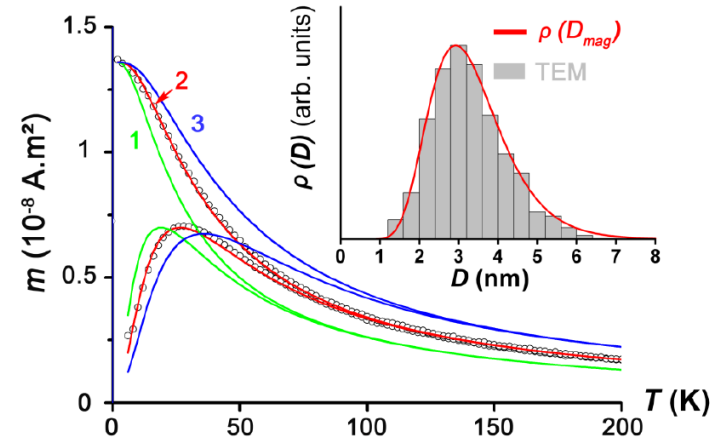


“Triple fit” = Superparamagnetic loop (300 K) + ZFC/FC curves

Simultaneous fit: the curves share common parameters (size distribution etc.)



Co particles diluted in Au.



Accurate determination of the magnetic anisotropy

Size selected CoPt nanoparticles (3 nm), as prepared

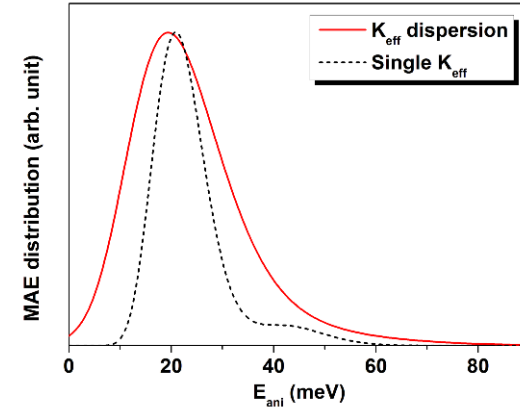
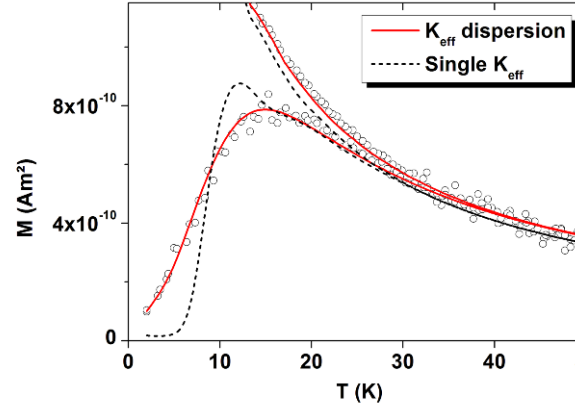
The usual $E_{ani} = K_{eff} V$ model is no more valid



Anisotropy constant dispersion

Gaussian distribution of K_{eff} :

- ✓ Relative dispersion ~ 40%
- ✓ $\langle K_{eff} \rangle \sim 200 \text{ kJ/m}^3$



Such a K_{eff} dispersion was not detectable for particles without size selection

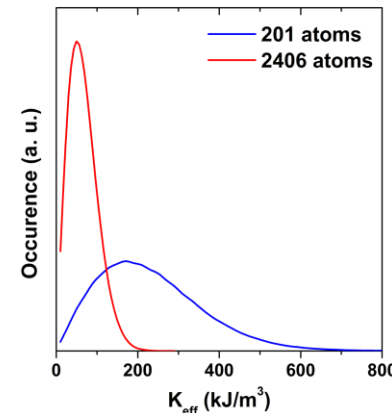
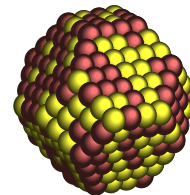


A narrow size distribution is necessary

Physical origin?

Nanoalloy effect

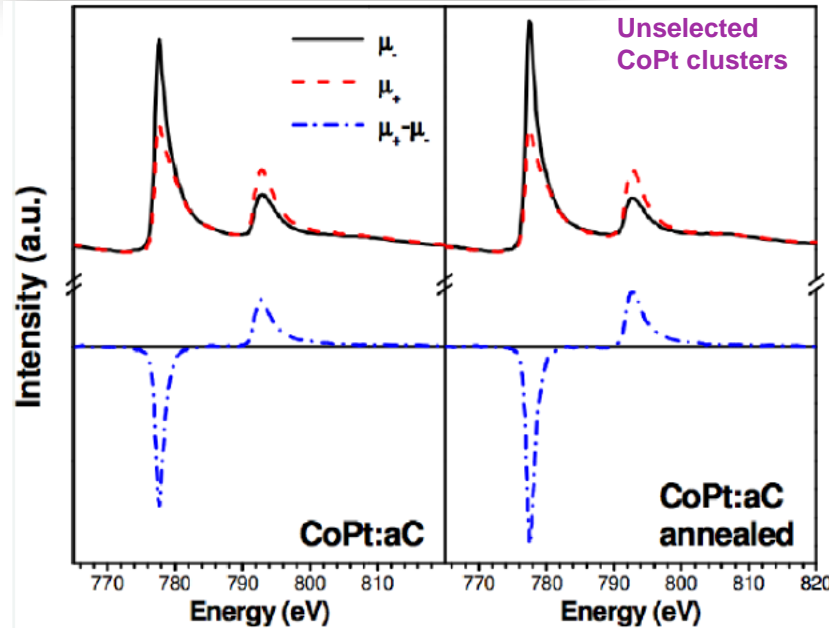
- ✓ Composition
- ✓ Chemical order
- ✓ **Atomic configuration**
(chemical arrangement)



K_{eff} distribution calculated for chemically disordered CoPt particles

Absorption at the Co L_{2,3} edge

➡ Co magnetic moments



As prepared

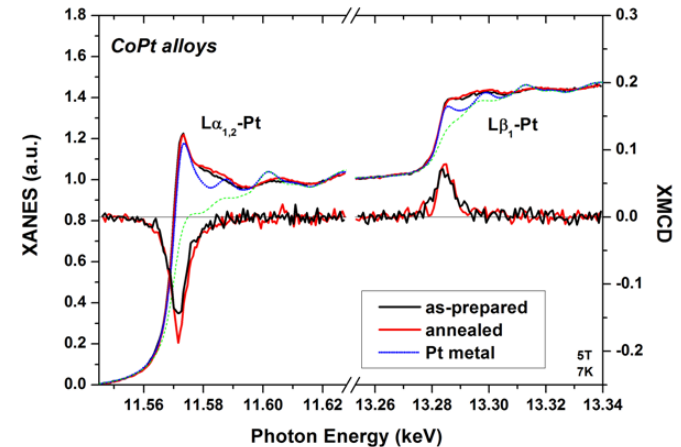
Annealed

	m_S	m_L	m_L/m_S
As prepared	1.70 μ_B/at	0.12 μ_B/at	0.071
Annealed	1.91 μ_B/at	0.18 μ_B/at	0.094

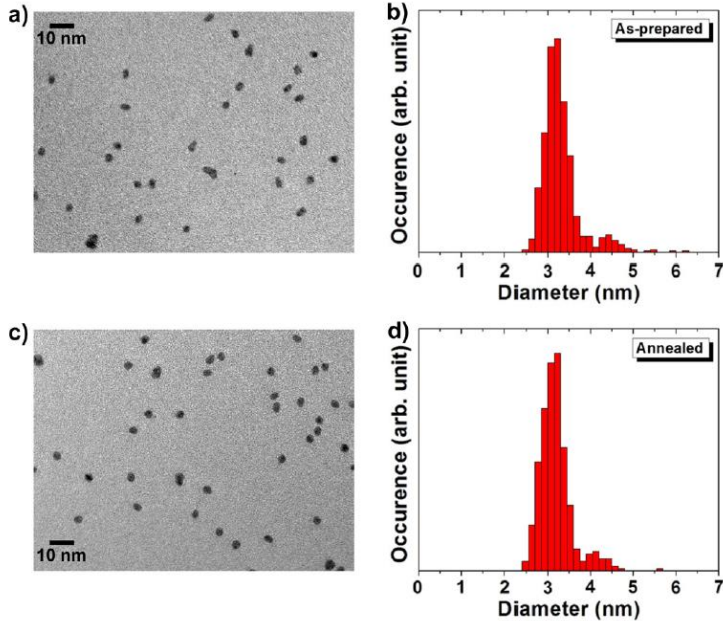
- ✓ No Co oxidation, no “dead layer”
- ✓ Very high m_S value (Co bulk = 1.6 μ_B/at)
- ✓ Increase of m_S , m_L and m_L/m_S upon annealing

Annealing induces a change of the magnetic moments

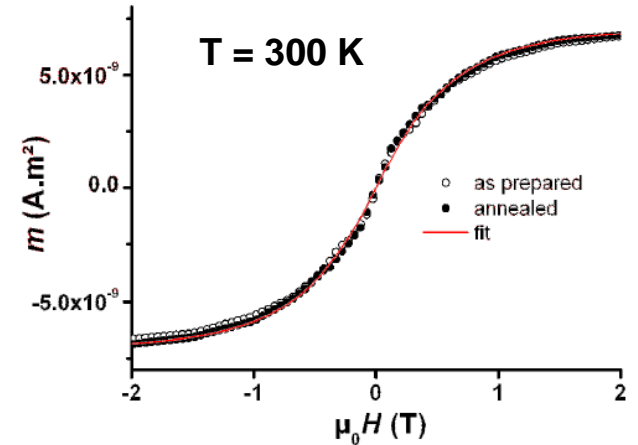
➡ A1 → L1₀ chemical ordering?



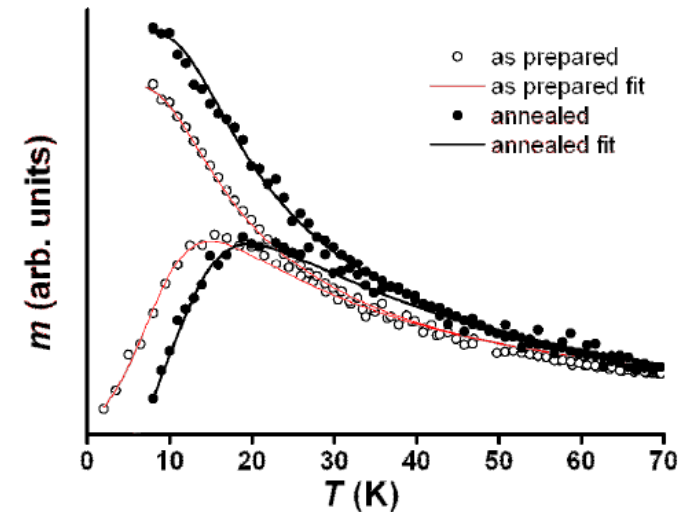
The Pt magnetic moment also increases (from 0.47 to 0.52 μ_B/at)



No modification of the particle size upon annealing



V. Dupuis *et al.*, IEEE Trans. Magn. **47**, 3358 (2011).



Evolution of the magnetic anisotropy

	As prepared	Annealed
D_m (nm)	3.12 ± 0.1	3.12 ± 0.1
ω (nm)	0.22 ± 0.05	0.22 ± 0.05
K_{eff} (kJ.m ⁻³)	218 ± 20	293 ± 30
ω_K (kJ.m ⁻³)	$37\% \pm 5\%$	$28\% \pm 5\%$

This increase is **much smaller** than what is observed in the bulk

To fix the ideas: with $K_{eff} = 5$ MJ/m³ and $D = 3$ nm $\rightarrow T_B = 200$ K

To go further: global fit, including a low T hysteresis loop.

➔ Significant biaxial contribution to the anisotropy.

	As prepared	Annealed (750 K)
D_m (nm)	3.12 ± 0.1	3.12 ± 0.1
σ (nm)	0.22 ± 0.05	0.22 ± 0.05
K_{1m} (kJ m ⁻³)	200 ± 25	260 ± 25
σ_{K1}/K_{1m}	$37\% \pm 5\%$	$31\% \pm 5\%$
K_2 (kJ m ⁻³)	100 ± 25	150 ± 25

Size-selected CoPt nanoparticles ($D = 3$ nm) embedded in amorphous C

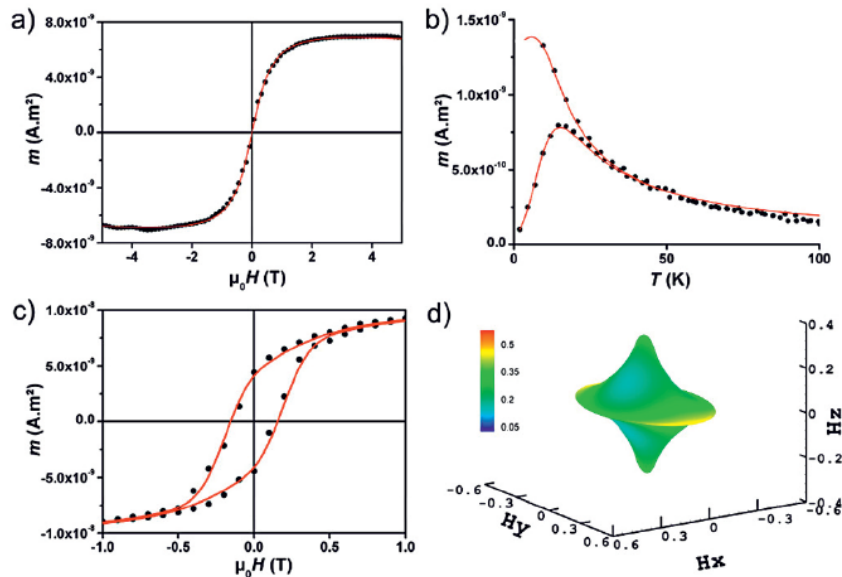


Fig. 3. (Color online) Hysteresis loops at 300 K (a), at 2 K (c) and ZFC/FC (b) for as-prepared CoPt nanoparticles embedded in C matrix. The solid lines correspond to the fit. Mean astroids associated to the biaxial fit (d).

As prepared

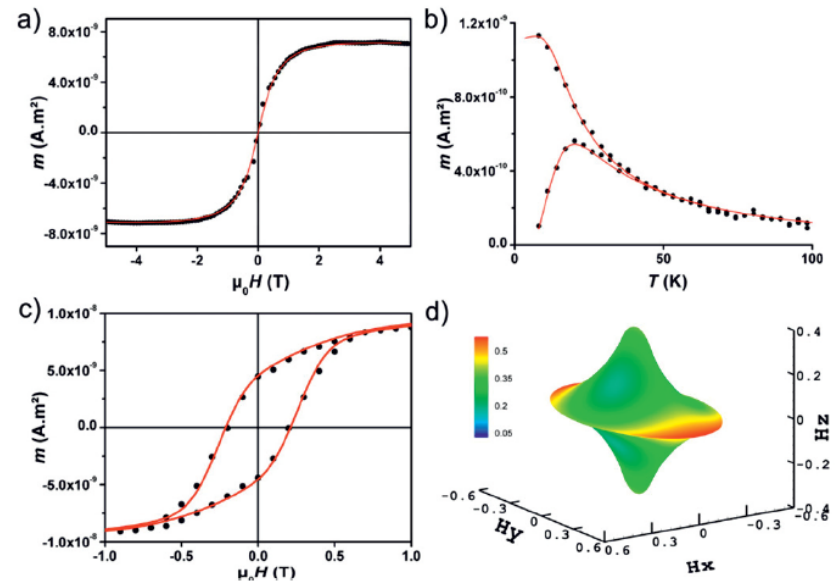


Fig. 4. (Color online) Hysteresis loops at 300 K (a), at 2 K (c) and ZFC/FC (b) for annealed CoPt nanoparticles embedded in C matrix. The solid lines correspond to the fit. Mean astroids associated to the biaxial fit (d).

Annealed

✓ **Structural characterization of CoPt particles in C**

- EXAFS measurements (Extended X-ray Absorption Fine Structure)
- HRTEM observations

EXAFS measurements:
probe the local environment
of one type of atoms

- Drastic change upon annealing
- Evolution of $N_{\text{Co}}/N_{\text{Pt}}$



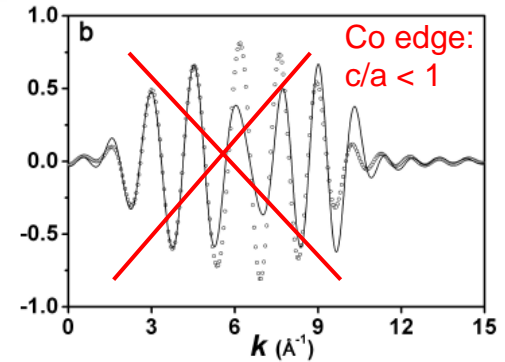
A1 → L1₀ transition

Apparent c/a ratio

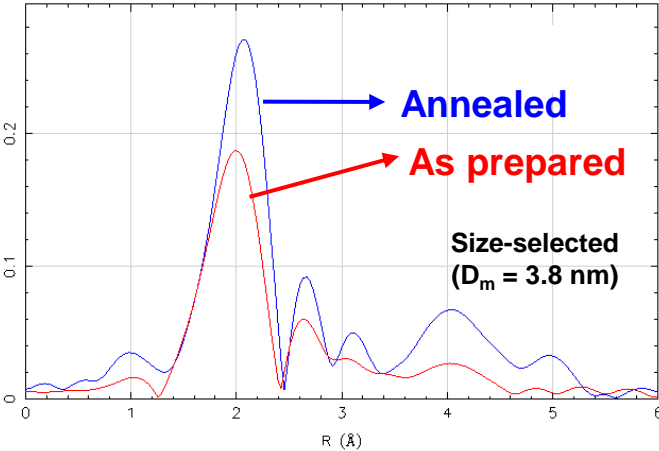
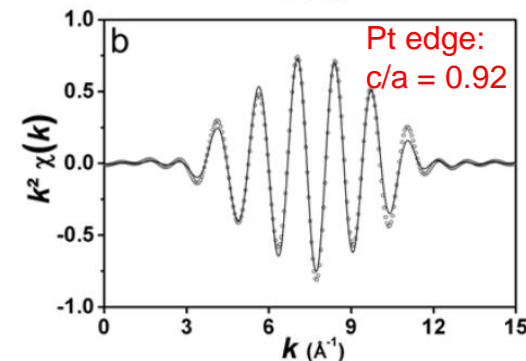
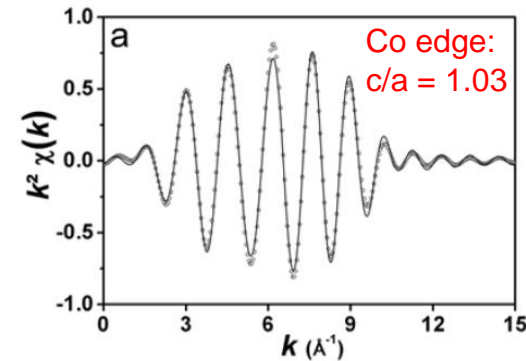


Different around Co
and Pt atoms:

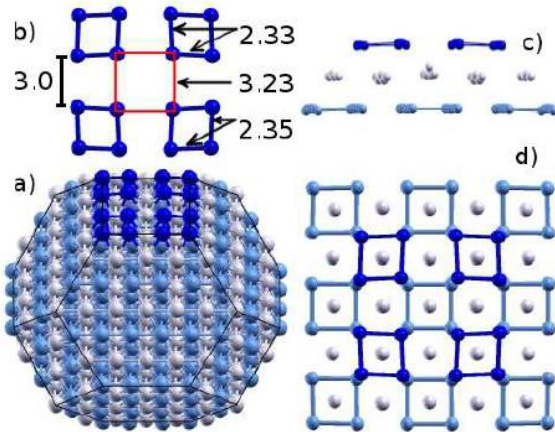
$$d_{\text{Pt-Pt}} \neq d_{\text{Co-Co}}$$



Tetragonalization
different from the bulk

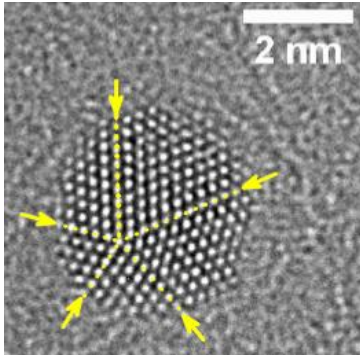


N. Blanc *et al.*, Phys. Rev. B **87**, 155412 (2013)
V. Dupuis *et al.*, Eur. Phys. J. B **86**, 1 (2013)

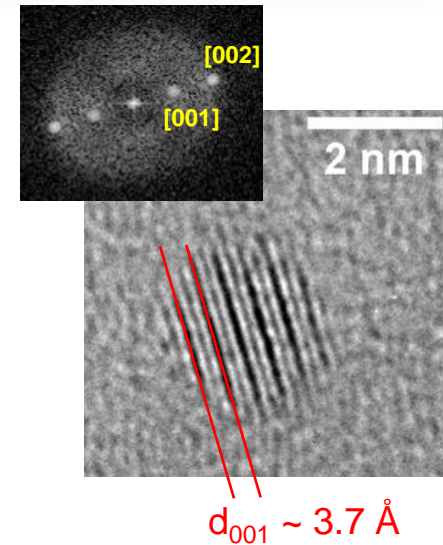


DFT calculations: “L1₀ like” structure

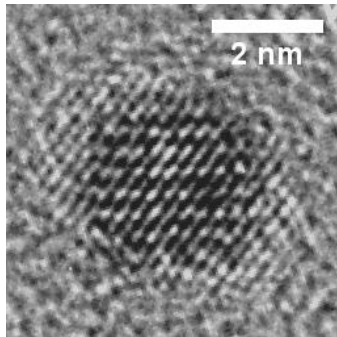
→ Strong relaxation of the Co-Co distances



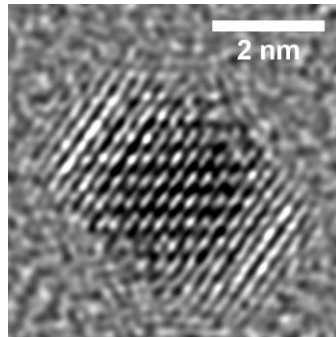
- ✓ Coexistence of fcc and multiply-twinned particles
- ✓ No chemical order before annealing
- ✓ L1₀ contrast ([001] peak) after annealing, even for the smallest particles



[110] orientation



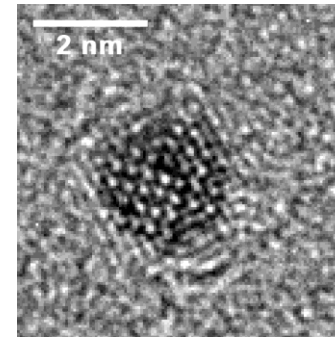
Exp.



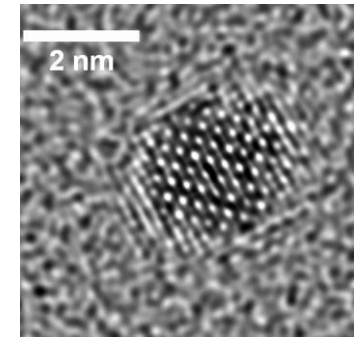
Simul.

**Experiment
vs.
simulations**

[001] orientation



Exp.



Simul.

But, chemical order is **not necessarily visible** (particle orientation, defocus) →

- ✓ Challenging observations!
- ✓ Not a statistical method

Method based on a simulation/experiment comparison

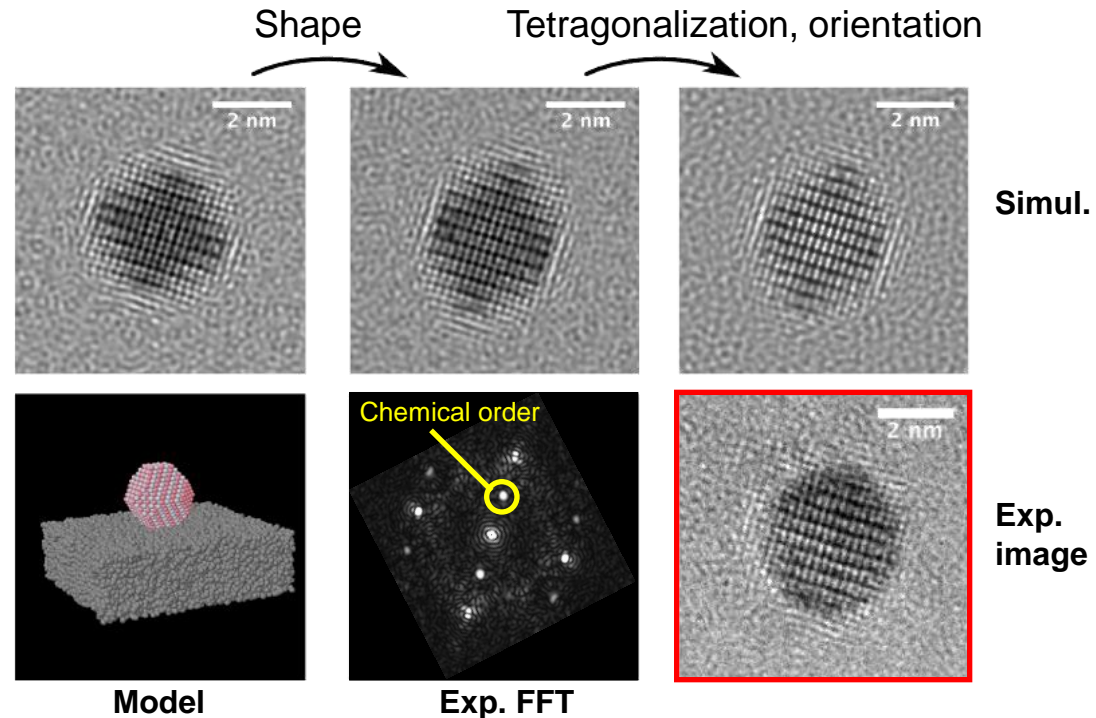
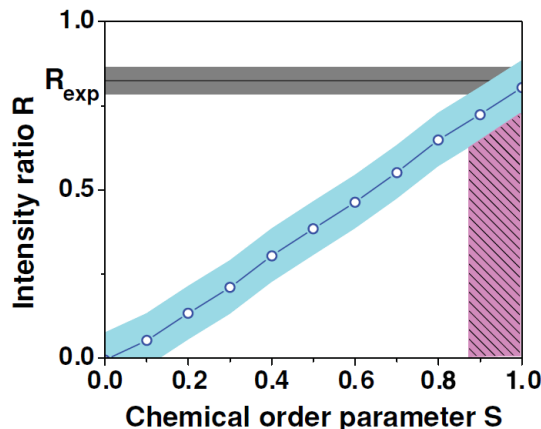
Determination of the imaging parameters and of the particle structure



Computed ratio between a chemical order peak and a structure peak (FFT)



Theoretical curve as a function of S



S value for the experimental image:
between 0.85 and 1

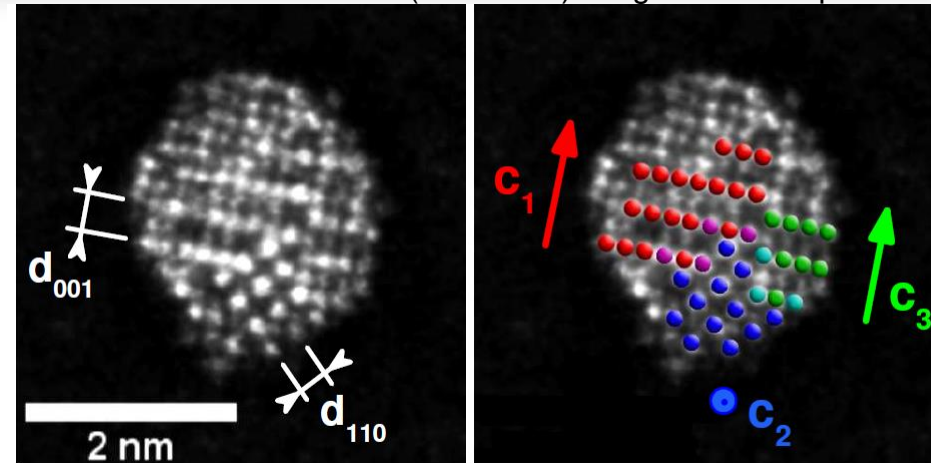
Limitations of the method: complexity,
uncertainty in a general case?

Coexistence of several L1₀ variants
(with antiphase boundaries)

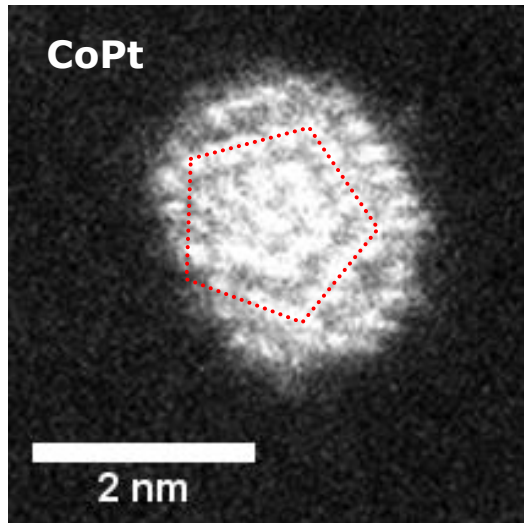


In a single-crystal
particle of 2 nm
diameter!

STEM HAADF (Z contrast) image of a CoPt particle



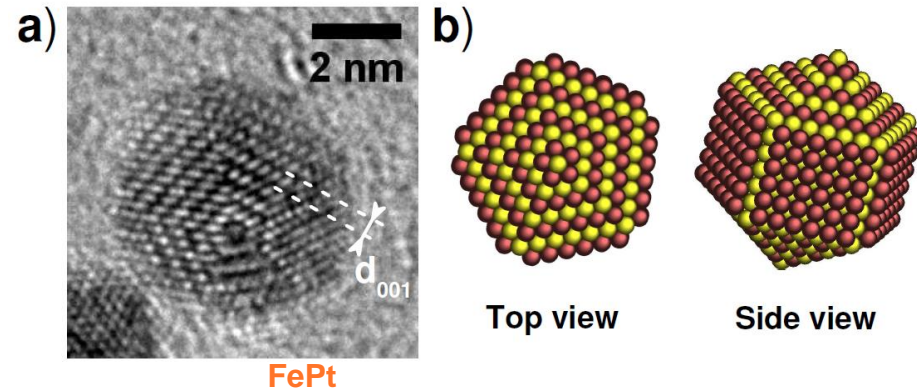
F. Tournus *et al.*, Phys. Rev. Lett. **110**, 055501 (2013).



Decahedral particles with a chemical order

➡ Five L1₀ domains with c axes in different directions

Theoretically
predicted
structure



STEM-HAADF image

Particles with several L1₀ domains



Lowering of the anisotropy!

Coexistence of various structures



Anisotropy constant dispersion

- ✓ Effort for the determination of the intrinsic properties of CoPt nanoparticles
 - ➡ Model systems, complementary characterizations

- ✓ Original properties of CoPt nanoparticles
 - Magnetic anisotropy dispersion, evolution of the atomic magnetic moments
 - For chemically ordered CoPt particles, the anisotropy remains much smaller than for the bulk $L1_0$ phase
 - Existence of structures with several $L1_0$ domains, “exotic” geometries
 - Relaxation of the inter-atomic distances because of finite size

- ✓ Similarities between CoPt and FePt nanoparticles
 - ➡ But completely different magnetic behavior!

Many open questions remain...

- Motivations
- Cluster deposition: originality of the LECBD technique
- CoPt nanoparticles: chemical order and magnetic anisotropy?
 - ✓ Magnetic measurements
 - ✓ Structural characterization
- **Self-organization of Pt based nanoparticles on C substrates**
 - ✓ **Clusters deposited on graphite and carbon nanotubes**
 - ✓ **Pt cluster organized on graphene/Ir(111)**
- Perspectives

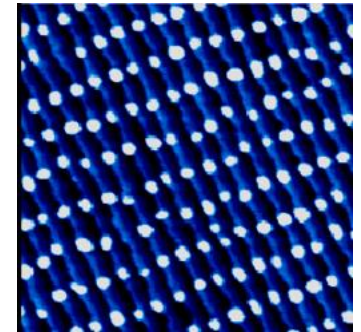
Applications: information storage...

Fundamental interest: inter-particle coupling, resonance effects...

Physical routes

- Atomic deposition on template surfaces (UHV conditions)
- Good organization for pure clusters
- Importance of the atom and particle/surface interaction

➔ Extension to bimetallic particles may be difficult



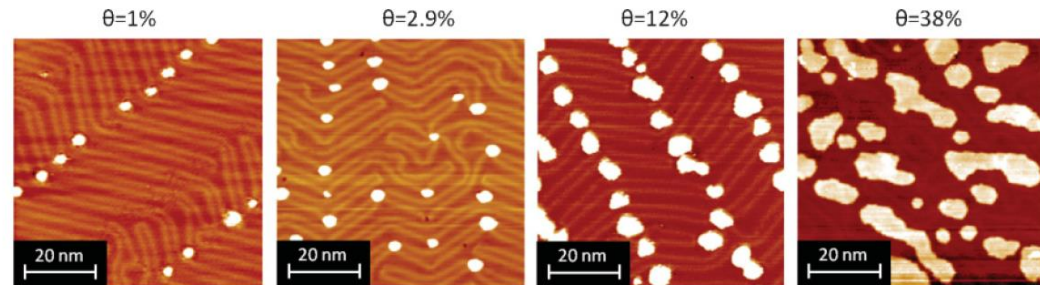
Co nanoparticles on Au(788)
V. Repain *et al.*
Euro. Phys. Lett. **58**, 730 (2002)

Preformed cluster deposition: an alternative approach

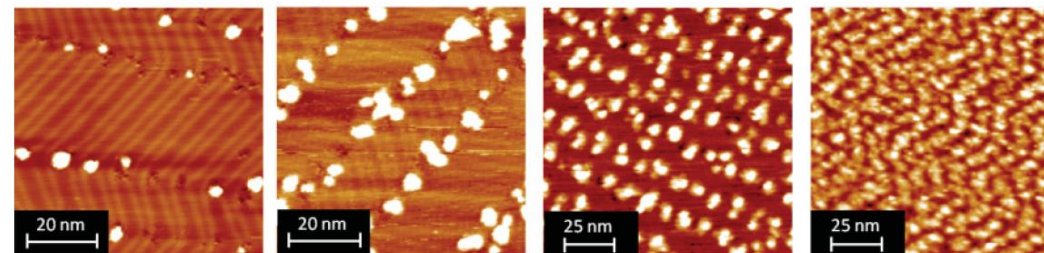


Not the same morphology
as with atomic deposition

Atomic
deposition



Cluster
deposition



Casari *et al.*, Phys. Rev. B
84, 155441 (2011)

$\theta=2.5\%$ (PLD, 5 shots)

$\theta=12.5\%$ (PLD, 20 shots)

$\theta=40\%$ (PLD, 100 shots)

$\theta=72\%$ (PLD, 300 shots)

Typical case of Au

High mobility of incident clusters

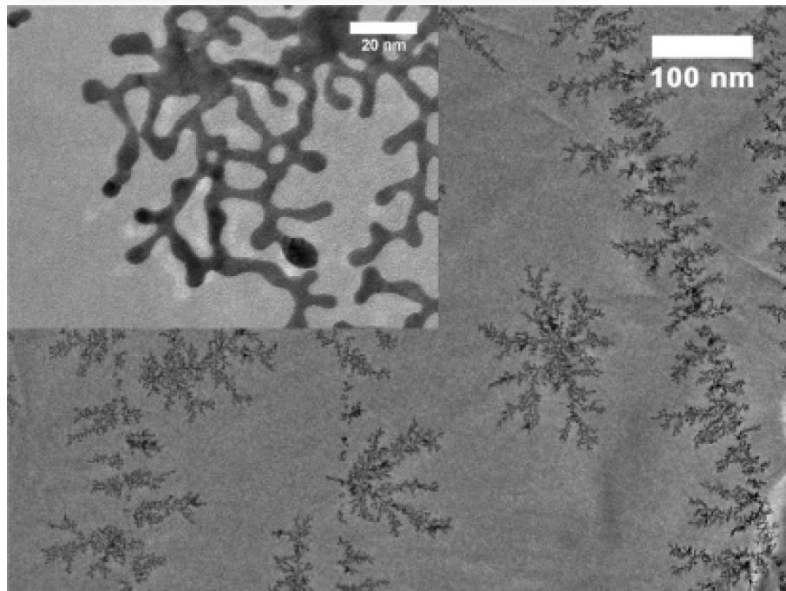
Ramified islands, with partial cluster coalescence

➡ Loss of the initial particle size

Processes involved:

Diffusion, nucleation, growth, coalescence

➡ This morphology is perfectly understood



2.2 nm Au clusters deposited on HOPG

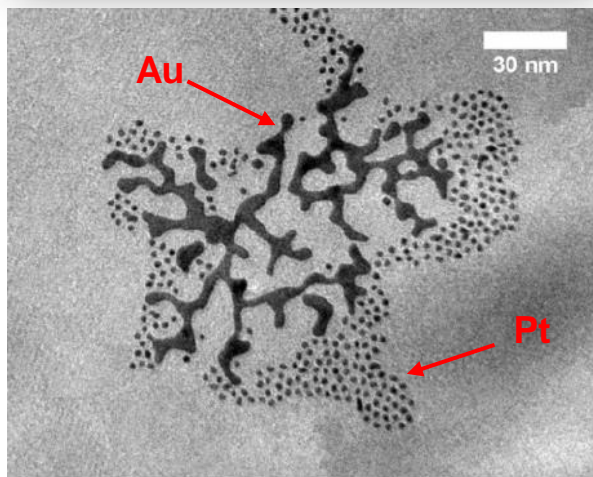
Characteristic timescales:

τ_{dep} time between two cluster landings on the surface
 τ_{diff} time for a cluster to diffuse on a distance d
 τ_{isl} time for a cluster to be captured by an island
 τ_{coal} time needed for the coalescence of two clusters

Control of the final morphology

Flux and temperature
(island density)

Temperature
(island shape)



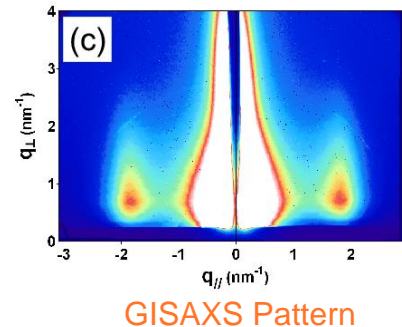
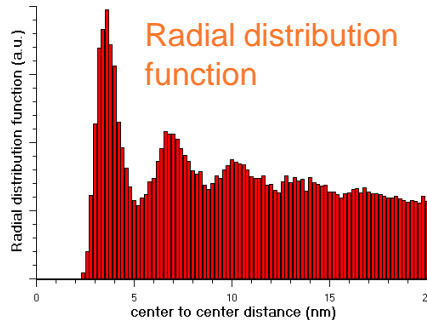
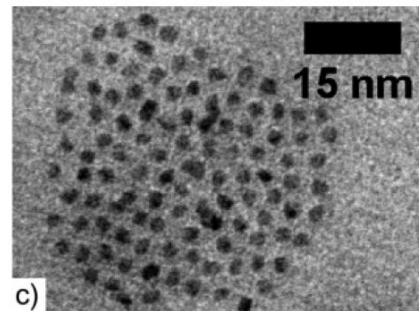
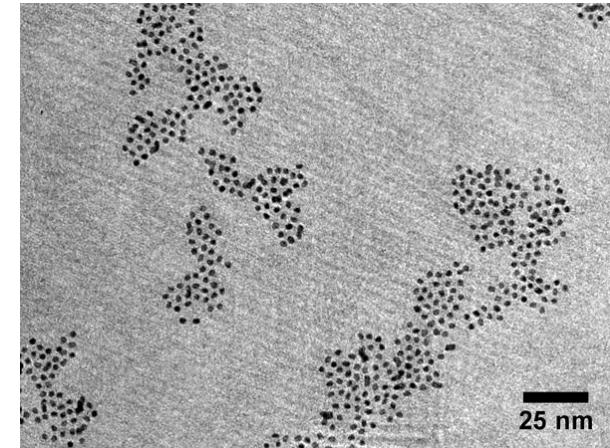
Successive deposition of Au and Pt clusters

Unusual behavior of Pt clusters!



No contact, no coalescence: the cluster size is preserved

Deposition of 2.2 nm Pt clusters



Local hexagonal order

Edge-to-edge distance well defined (~ 1.2 nm)

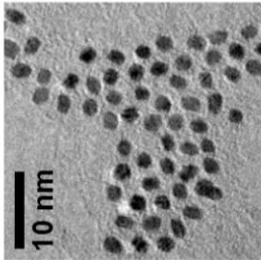
This can be explained by a surface reactivity: passivation effect with residual CO.

τ_{pass} time needed for cluster surface passivation

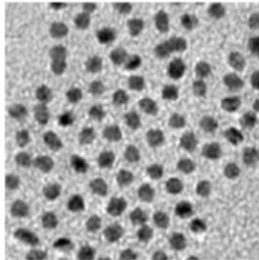
➡ **New parameter to control the cluster layer morphology**

Specific morphology of platinum in UHV attributed to its very high reactivity

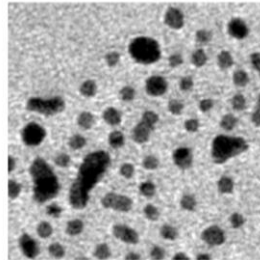
Pt



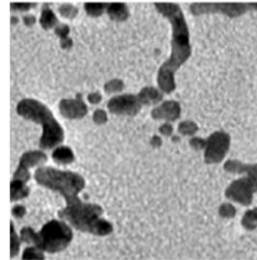
$Au_{0.2}Pt_{0.8}$



$Au_{0.5}Pt_{0.5}$

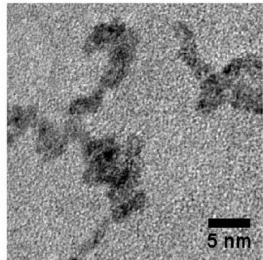


Au

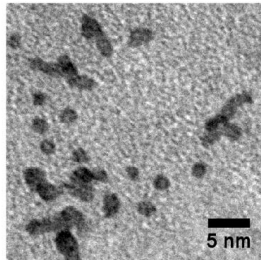


Au_xPt_{1-x}

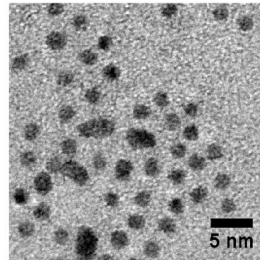
Bardotti et al., Surf. Sci. **606**,
110 (2012)



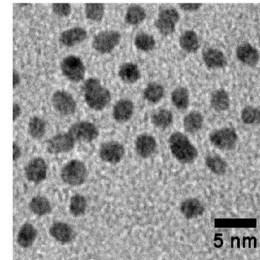
Co



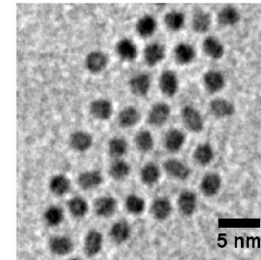
Co_3Pt



CoPt

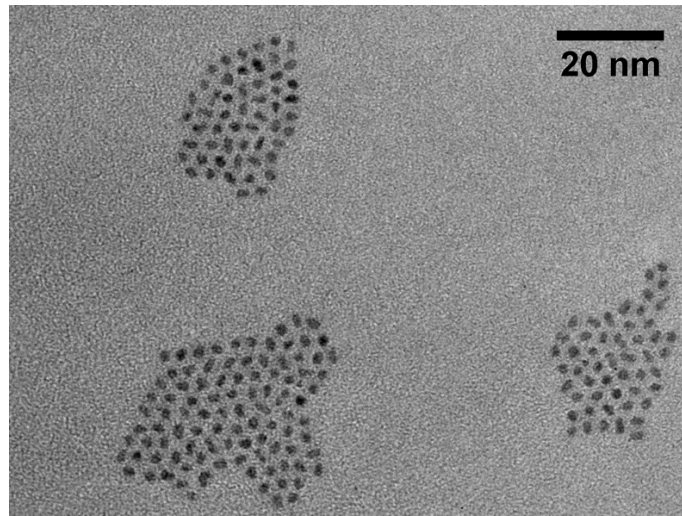


$CoPt_3$



Pt

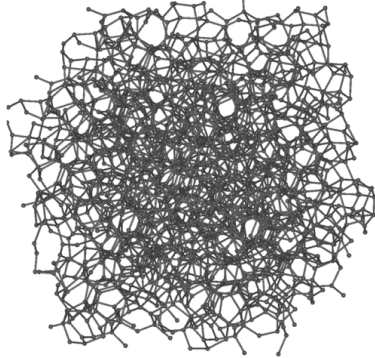
Co_xPt_{1-x}



FePt

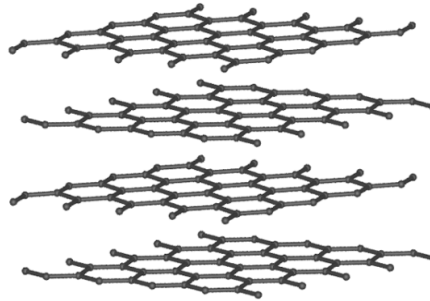
Decrease of τ_{pass} with increasing Pt content.

Amorphous carbon (a-C)



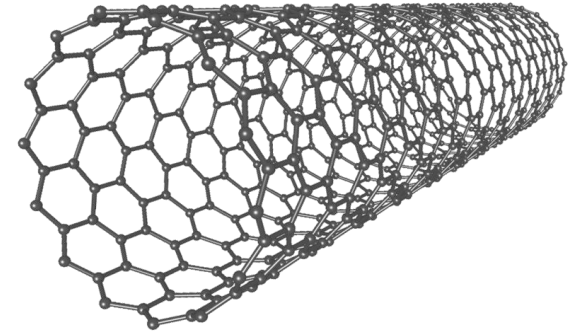
No diffusion

Graphite (HOPG)



Diffusion

Carbon nanotube (CNT)



Diffusion? Self-organization?

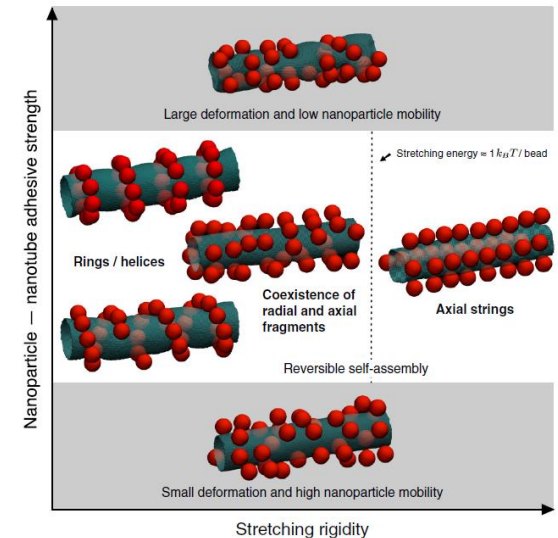
Technological interest

➔ Nanotube functionalization, sensors, catalysis, fuel cells...

Open fundamental questions

➔ Cluster/surface interaction
Curvature: anisotropy of the diffusion?

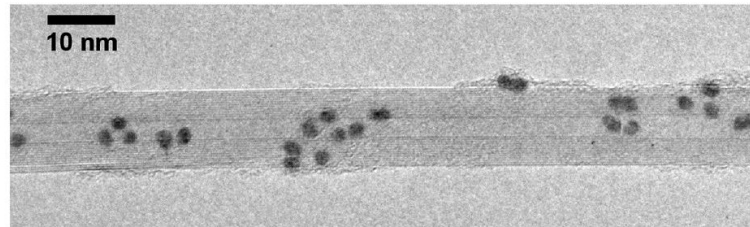
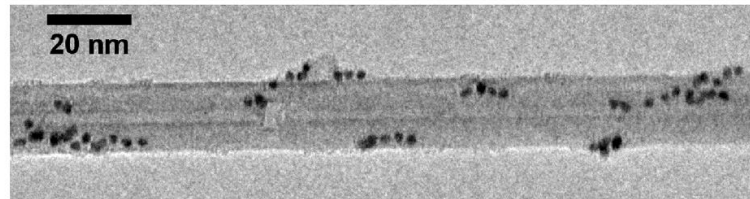
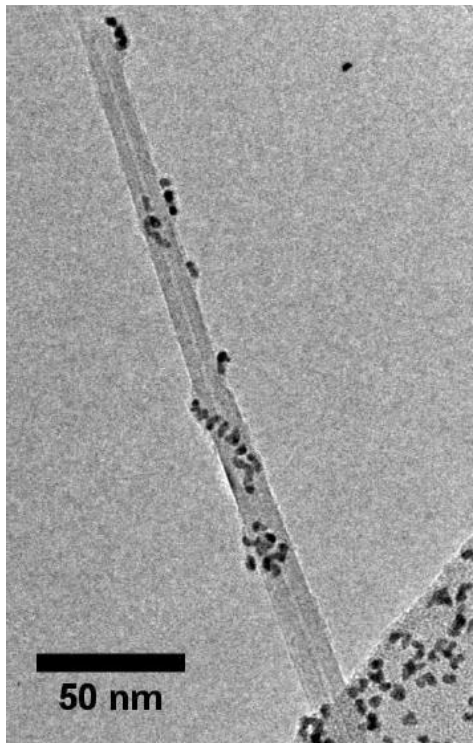
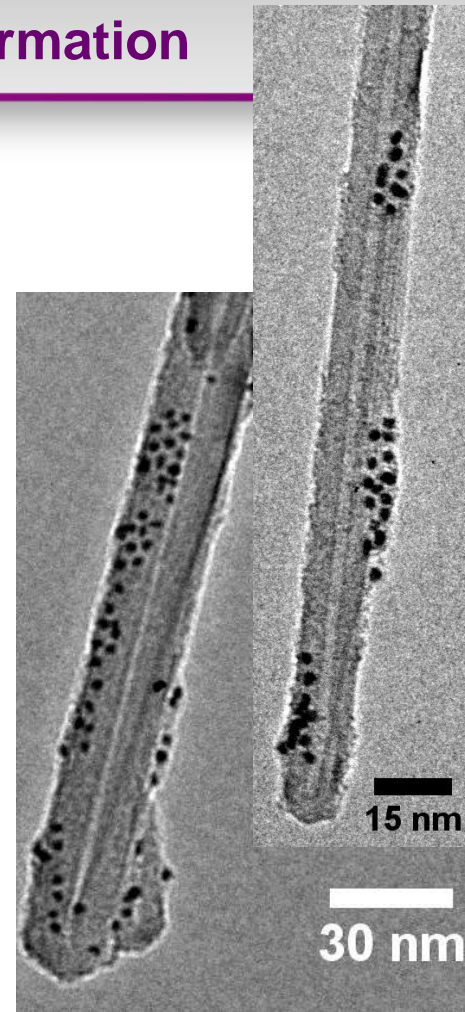
Preformed cluster deposition ➔ Model system



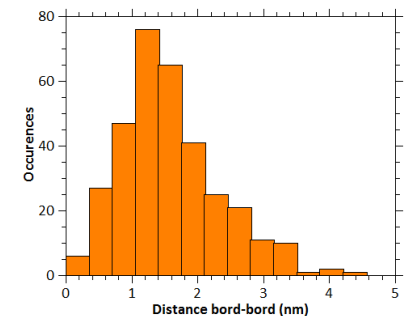
Deposition of size-selected FePt clusters on multiwall CNT (electric-arc synthesis)

The incident clusters diffuse on the CNT surface

➔ Formation of “bunches” of clusters

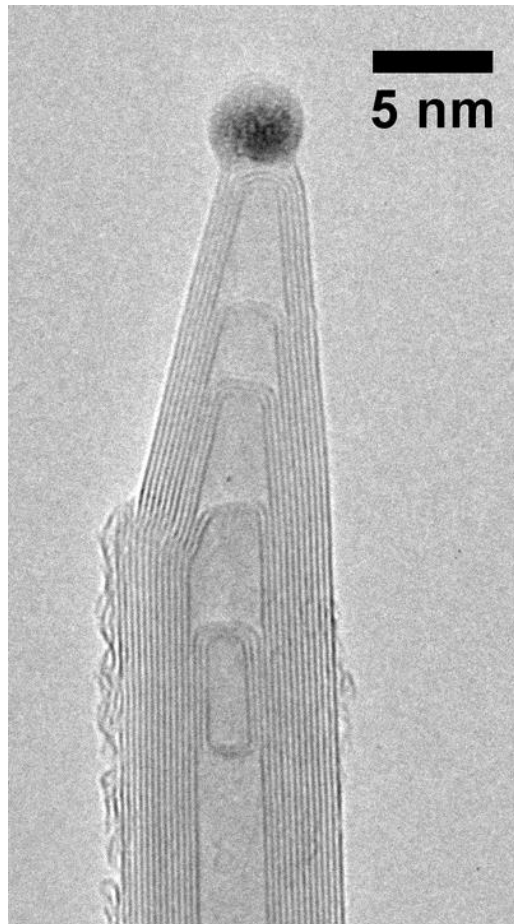


Inter-particle distance compatible with what is observed on HOPG

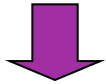


L. Bardotti *et al.*, *Appl. Surf. Sci.* (2014), in press.

Tube apex and changes of curvature act as pinning sites

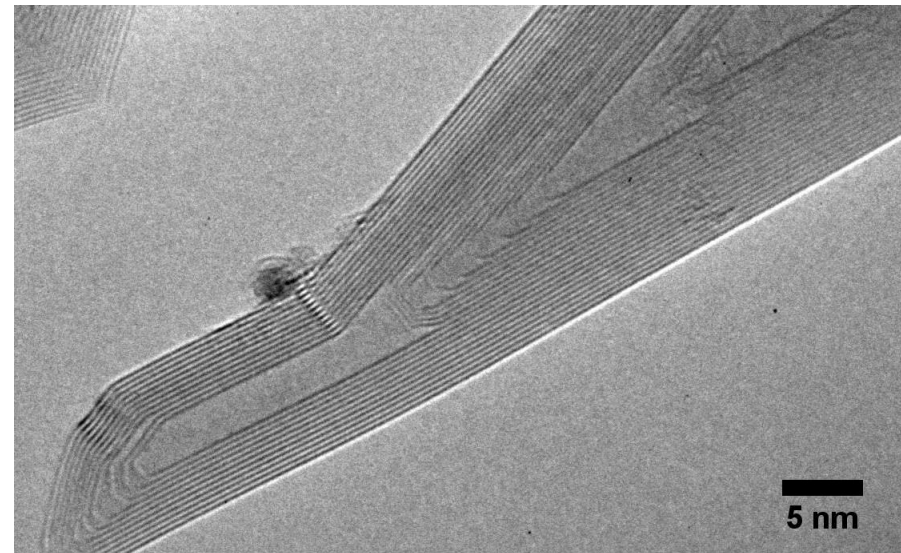
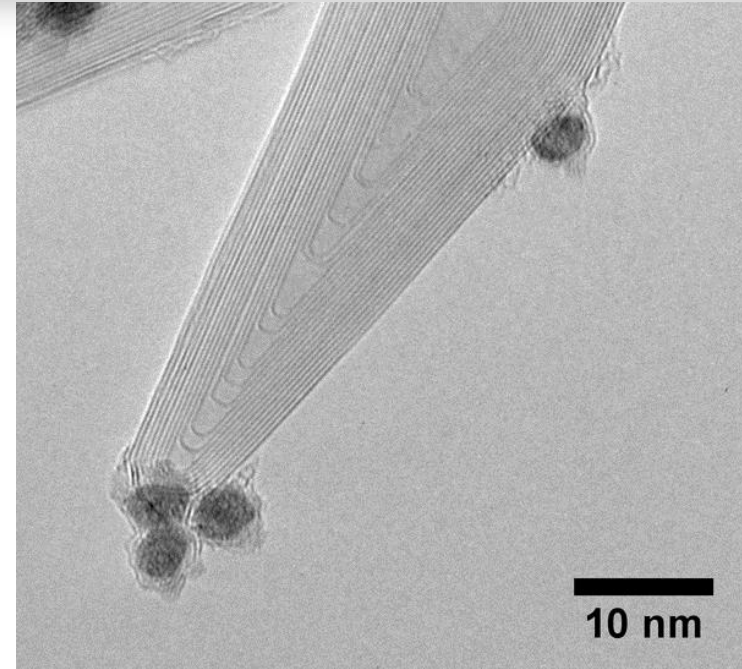


Defects

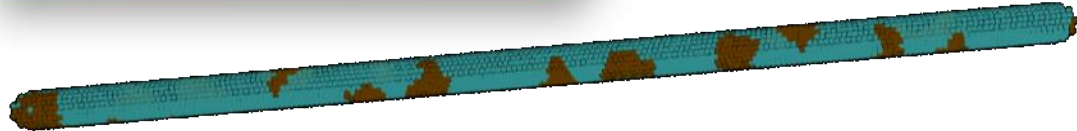


Enhanced
particle/CNT
interaction

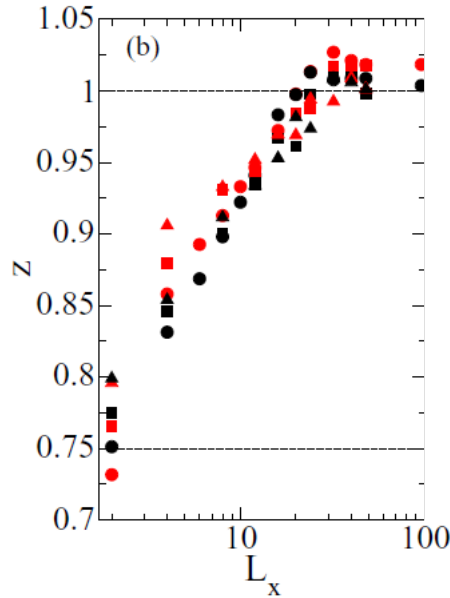
Potentially
interesting...



Kinetic monte-carlo simulations.

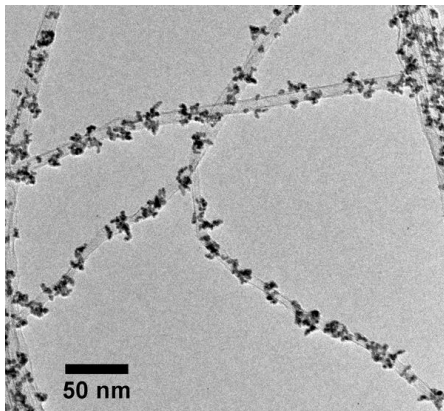
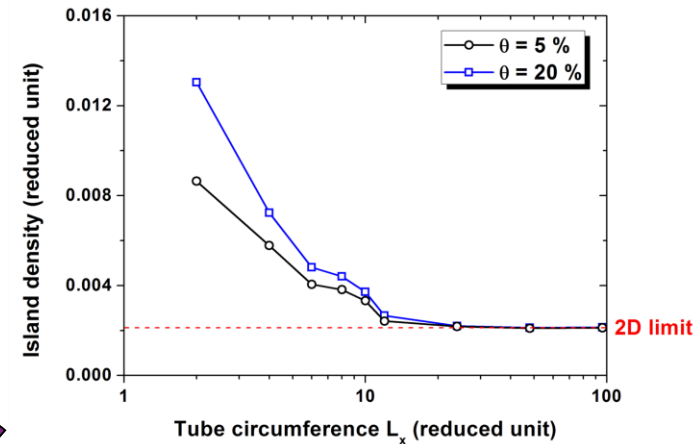


Transition from 2D to 1D behavior.



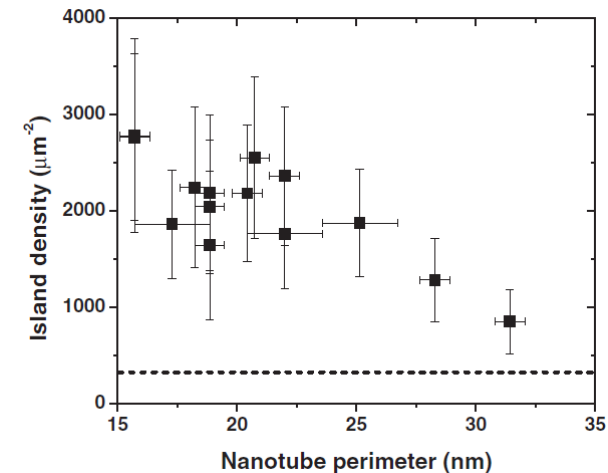
$$N \sim \theta^{1-z} R^{-\chi}$$

↓ Island density
 ↓ Surface coverage
 ↓ Deposition rate



Higher island density for small diameter nanotubes.

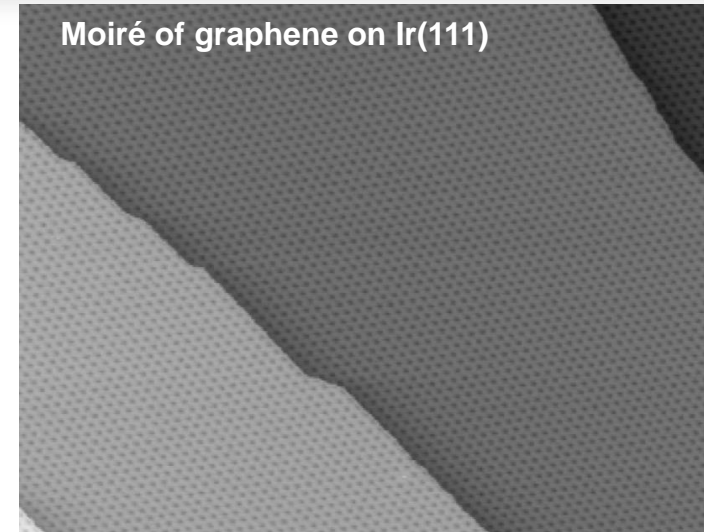
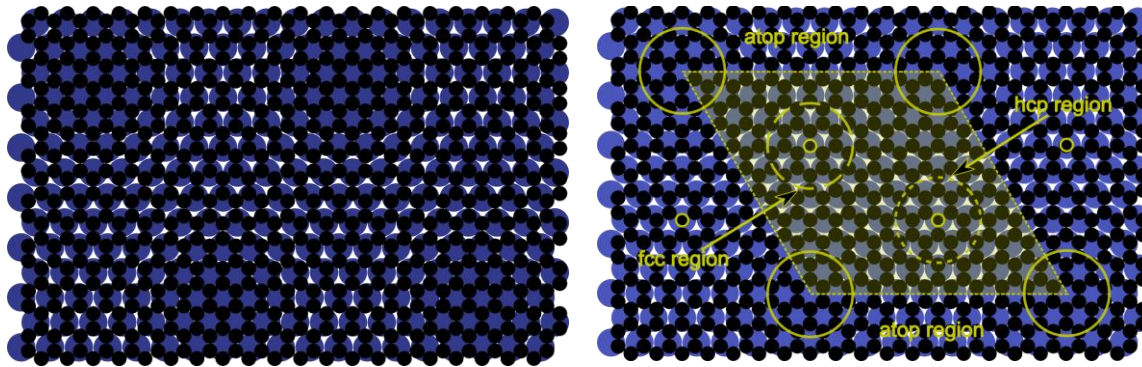
Experimental observations consistent with the theoretical prediction.



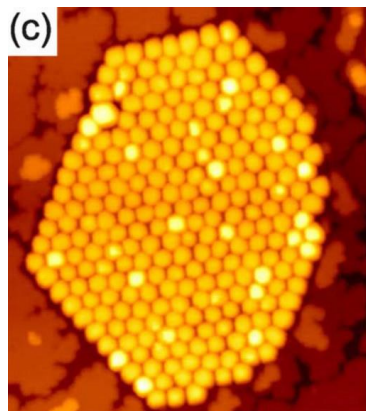
Idea: use the **moiré lattice** of graphene epitaxially grown on Ir(111) to obtain **arrays of particles**

Lattice mismatch produces a moiré

➔ specific sites with a 2.5 nm periodicity



J. Coraux *et al.*, *Nano Letters* **8**, 565 (2008).



✓ Organized growth of dots with atomic deposition

✓ Self-organization using deposition of preformed clusters?

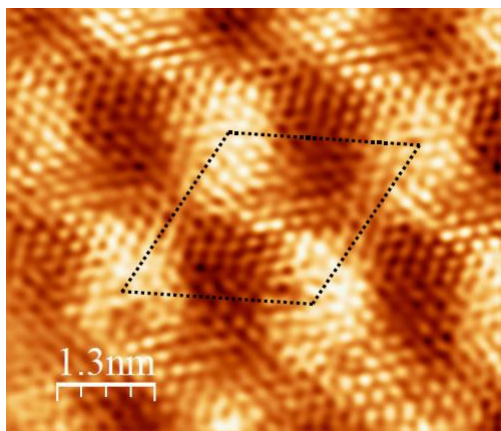
➔ Deposition of Pt clusters (1.5 nm).

N'Diaye *et al.*, *New J. Phys.* **11**, 103045 (2009); *Phys. Rev. Lett.* **97**, 215501 (2006).

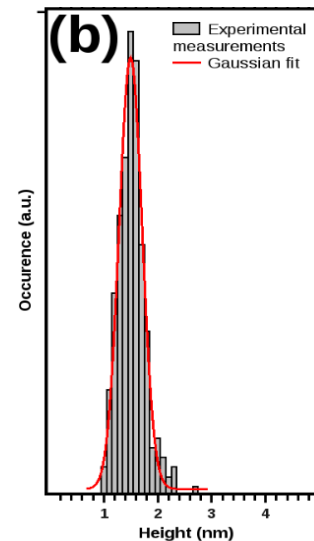
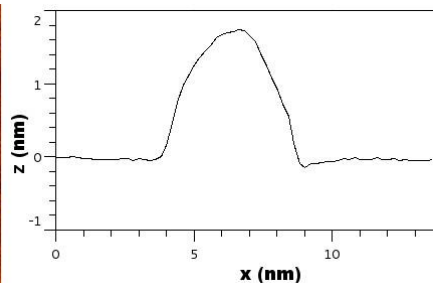
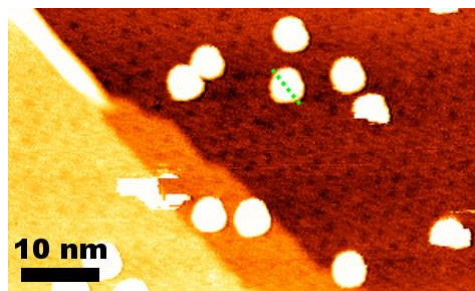
Collaboration with G. Renaud

Room temperature deposition of size-selected Pt clusters

✓ In situ **STM observations.**

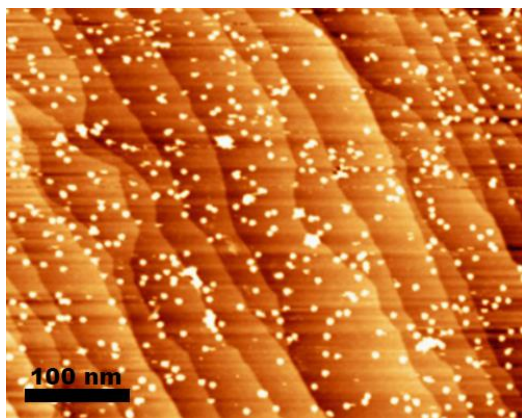


Moiré of the bare graphene/Ir(111) surface.

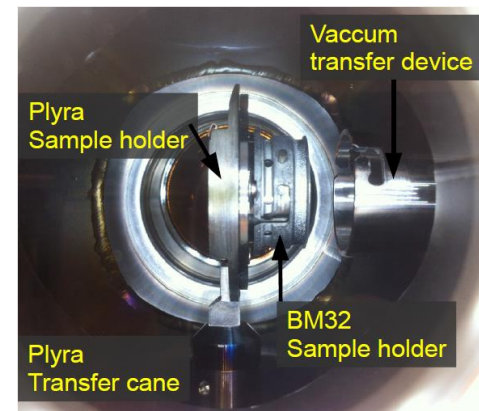
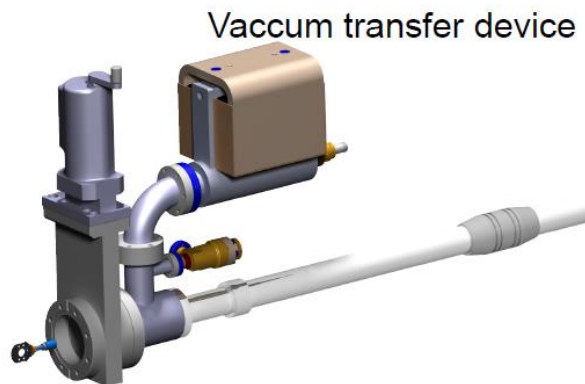


➔ Low diffusion of the clusters.

✓ **X-ray experiments** at ESRF with UHV transfer from Lyon to Grenoble.

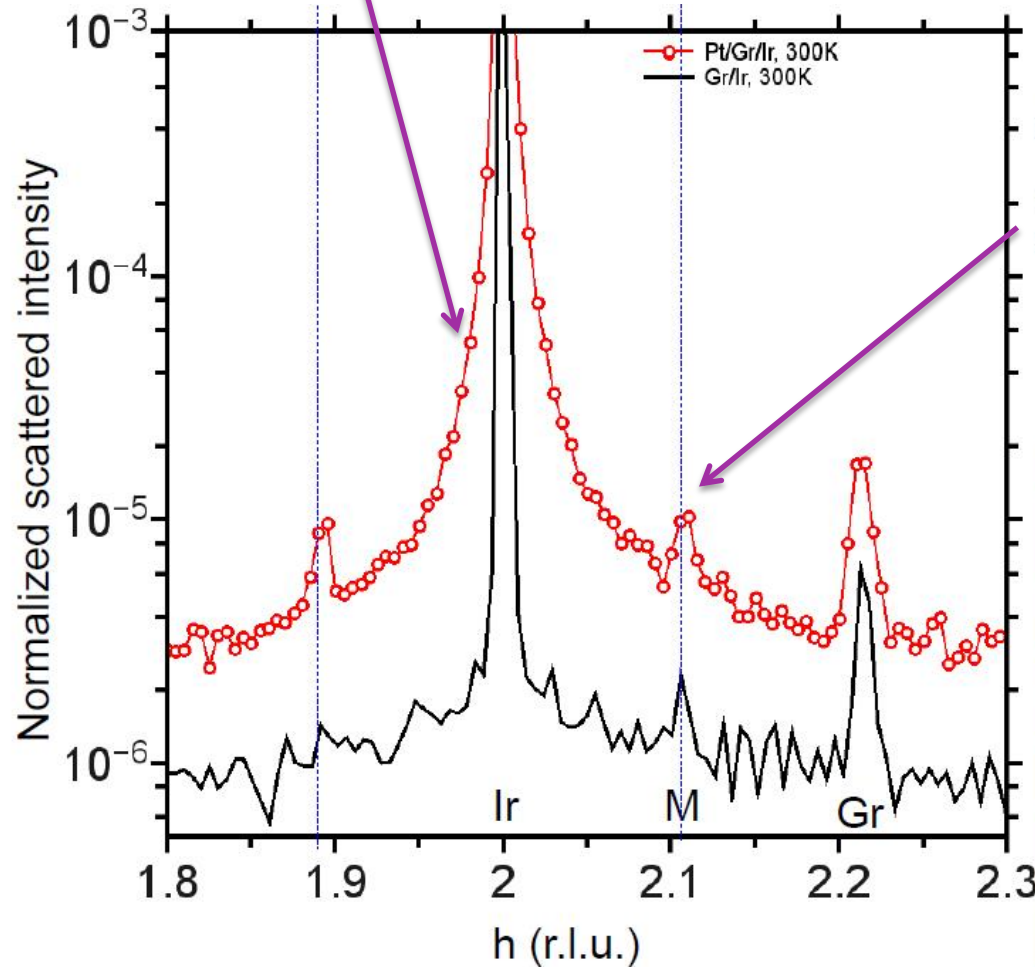


After Pt cluster deposition (low coverage).



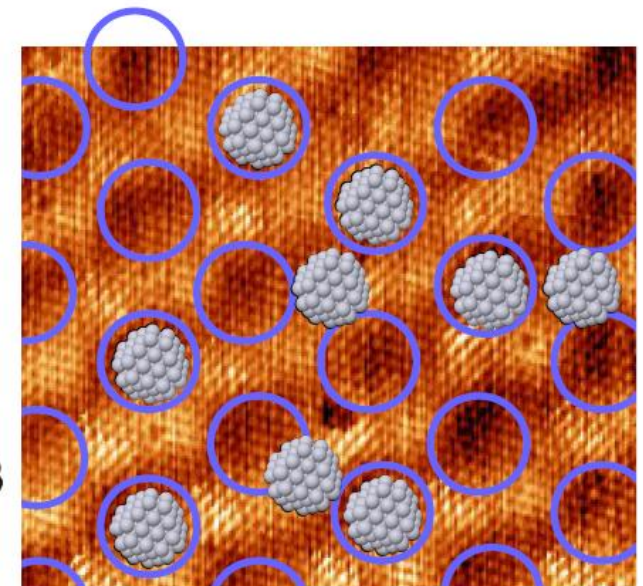
Grazing incidence XRD at ESRF (BM32 beamline).

Pt particles on epitaxy with the Ir substrate

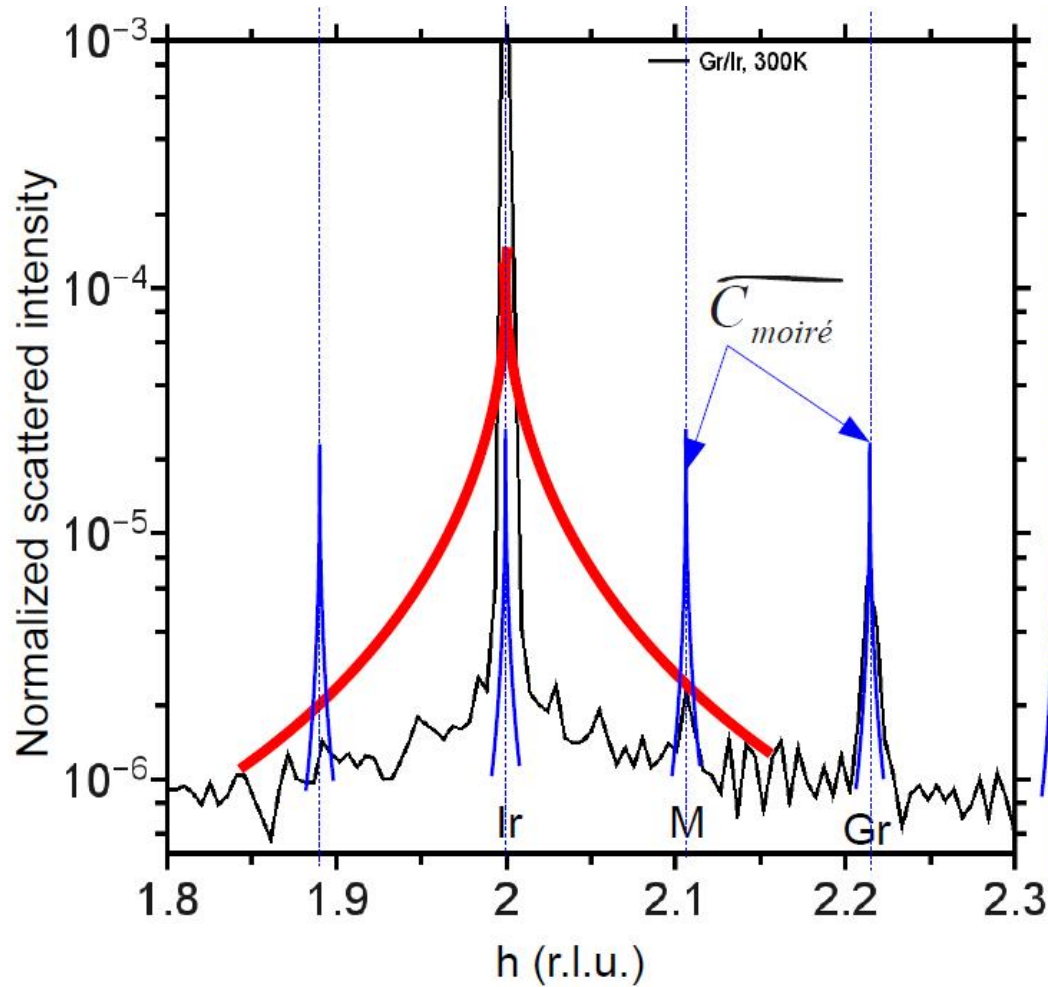


Some particles are randomly distributed

Some particles are pinned on a specific moiré site



Curves shifted for the eyes



- Particles in **epitaxy**, randomly distributed

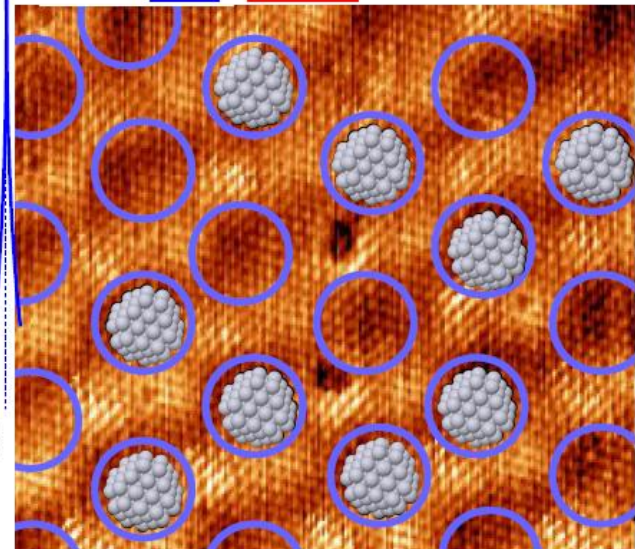
$$N = F \times C_{Pt}$$

$$I = \widetilde{F} \otimes \widetilde{C}_{Pt} \quad \blacktriangleright \text{Broadening of the Ir peak}$$

- Particles in **epitaxy**, pinned on the moiré lattice

$$N = C_{\text{moiré}} \otimes (F \times C_{Pt})$$

$$I = \widetilde{C}_{\text{moiré}} \times (\widetilde{F} \otimes \widetilde{C}_{Pt})$$



Grazing Incidence Small Angle Scattering (Decoupling approximation)

$$I(\mathbf{q}) = |\langle F(\mathbf{q}) \rangle|^2 \times S(\mathbf{q}) + \underbrace{|\langle F(\mathbf{q})|^2 \rangle - |\langle F(\mathbf{q}) \rangle|^2}_{\text{Diffusive term}}$$

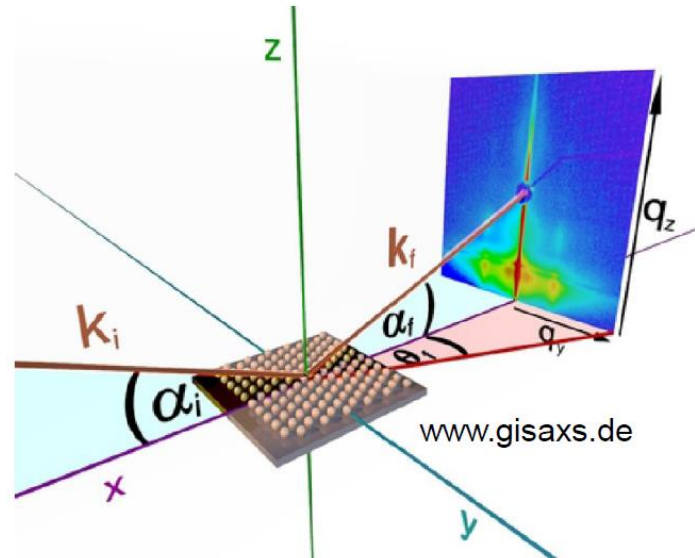
Diffusive term

$I(\mathbf{q})$: Scattered Intensity

$F(\mathbf{q})$: Form factor

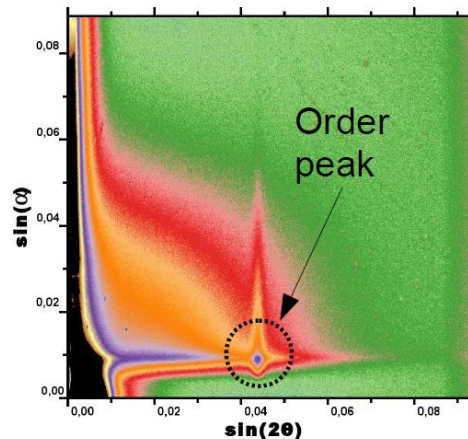
$S(\mathbf{q})$: Interference function

Information about the shape and distribution of nanostructures.

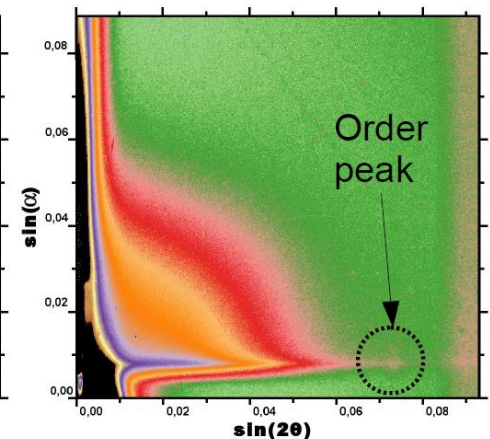


Hexagonal lattice of Pt clusters
(lattice parameter = 2.5 nm)

➔ Pt clusters pinned on a specific moiré site!



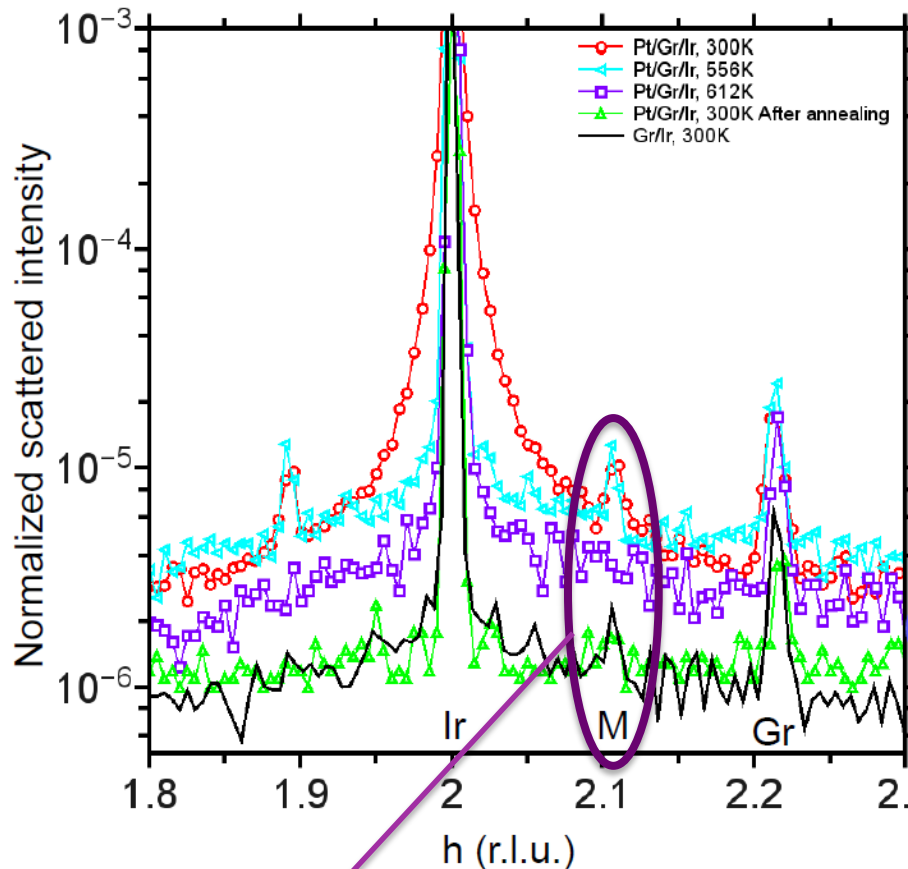
Ir [100]



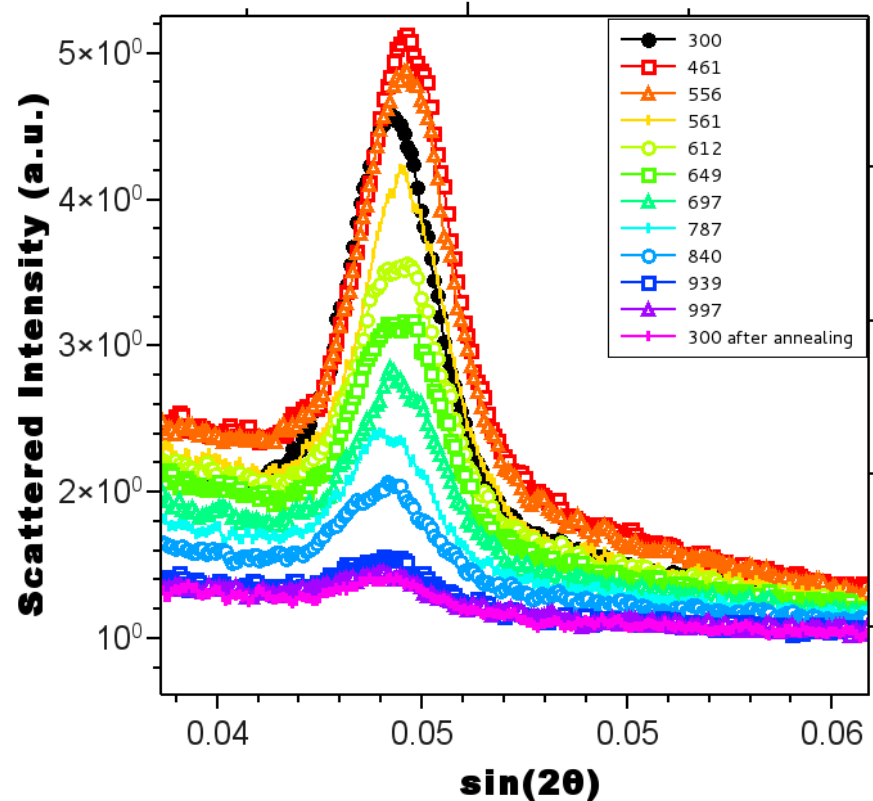
Ir [110]

Signature of the particle organization:

- Moiré peak in GIXRD (epitaxy is required)
- Order peak in GISAXS (no epitaxy needed)

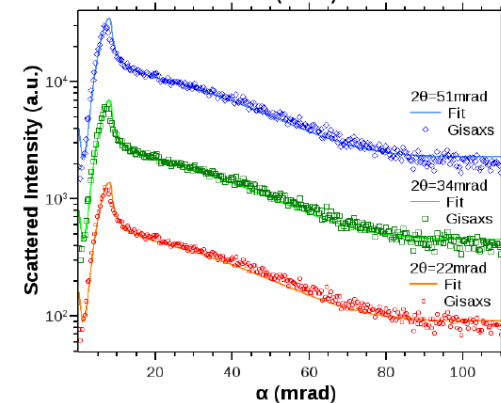
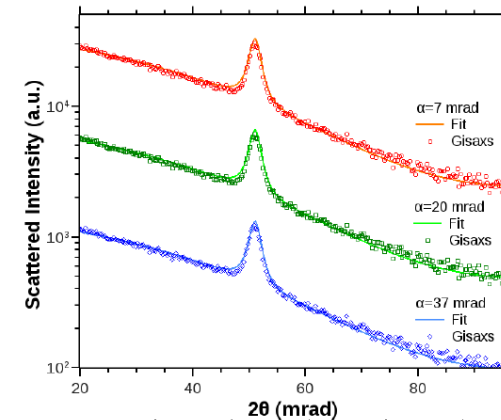
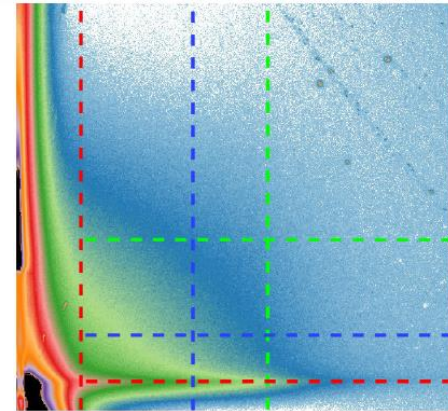


No more moiré peak for T= 612 K



Pt particles are still organized for T = 612 K, without change of size.

- ✓ Self-organization of preformed Pt clusters at room temperature, stable up to around 600 K.
- ✓ Epitaxy with the Ir surface
- ✓ Efficient pinning at moiré sites
 - ➡ Upon annealing, epitaxy is lost before the lattice order.
- ✓ Quantitative analysis of the proportion of clusters on the moiré lattice
 - ➡ GISAXS simulations needed (ongoing work).
- ✓ Deposition of FePt clusters on graphene
 - ➡ Interesting for magnetism.



- Self-organization of nano-magnets (deposition on template surfaces).
- Understand size reduction effects in magnetic nanoalloys (exotic structures, magnetic transitions).
- Multifunctional systems (plasmonics, reactivity).
- Single particle measurements (XPEEM, transport, STM, microSQUID...)
- Superconducting clusters

Groupe « Nanostructures magnétiques » :

L. Bardotti
V. Dupuis
G. Khadra (Thèse)
S. Linas (Post-Doc)
A. Tamion
F. Tournus
J. Tuaille-Combes

N. Blanc (Thèse soutenue en 2009)
A. Hillion (Thèse soutenue en 2012)

Ingénieurs et support technique :

C. Albin
O. Boisron
G. Suteau

Plateformes : PLYRA, CML, CLYM



Centre de Magnétométrie de Lyon

T. Epicier (MATEIS, INSA Lyon)
K. Sato (IMR, Tohoku University, Japon)
T. J. Konno (IMR, Tohoku University, Japon)



G. M. Pastor (Universität Kassel)
L. E. Díaz-Sánchez (Univ. Autónoma del Estado de México)

A. Y. Ramos (Institut Néel, Grenoble)
H. C. N. Tolentino (Institut Néel, Grenoble)
M. De Santis (Institut Néel, Grenoble)
O. Proux (Obs. Sci. de l'Univers, Grenoble)

A. Rogalev (ESRF synchrotron)
F. Wilhelm (ESRF synchrotron)
P. Ohresser (SOLEIL synchrotron)

G. Renaud (CEA Grenoble/ESRF)
F. Jean (Institut Néel, Grenoble)



O. Pierre-Louis (ILM, Lyon)
R. Delagrangé (ILM Lyon, stage M1)
J.-M. Benoît (ILM, Lyon)
M. Hillenkamp (ILM, Lyon)

Réseaux :

